Impacts of species differences in drug metabolizing enzymes on human bioavailability prediction

(ヒトのバイオアベイラビリティ予測における薬物代謝酵素の種差の影響に関する研究)

2012

Takafumi Akabane

赤羽 隆文

Contents

Introduction;

Given the high costs and labor-intensive efforts involved in the development of a new drug, selection of candidates with good pharmacokinetic profiles is becoming commonplace (Wishart 2007). Indeed, while poor exposure of candidate compounds was the most significant cause of attrition, accounting for approximately 40% of all candidate loss in the early 1990s, the contribution of poor pharmacokinetics to all attrition had dramatically decreased to less than 10% by 2000 due to improvements in methods for predicting human pharmacokinetics, including development of the physiological model, well-stirred model, parallel tube model, and dispersion model (Iwatsubo et al., 1996, Naritomi et al., 2001, De Buck et al., 2007). In addition, human liver microsomes became commercially available in the late 1990s, and screening systems to evaluate metabolic stability toward cytochrome P-450 (CYP)-mediated metabolism in the liver have also been developed, facilitating selection of drug candidates most stable against CYP metabolism in the liver. In contrast, increasing focus is being directed towards the role of extra-hepatic or non-CYP metabolism in elimination of drug candidates from the body (Doherty and Charman 2002, Williams et al., 2004).

The intestine is the major organ involved in extra-hepatic metabolism in the body, and members of the CYP3A subfamily are present in high levels in human intestinal epithelial cells as metabolizing enzymes, influencing the oral exposure of several drugs (Doherty and Charman 2002). Benet et al. (1999) proposed that the synergistic effects of CYP3A4-mediated metabolism and p-glycoprotein (P-gp)-mediated efflux in epithelial cells may result in unexpectedly high first-pass metabolism in

the intestine due to the overlapping substrate specificities of these proteins. Therefore, when predicting human pharmacokinetics, the fraction absorbed (Fa) and intestinal availability (Fg), in addition to hepatic availability (Fh), are the main factors to consider. However, unlike Fh, which can be easily estimated via conventional pharmacokinetic analysis described above, Fa and Fg are difficult to evaluate separately. As such, animal pharmacokinetic parameters have mainly used to predict human FaFg in the drug discovery stage.

Similarly, an increasing amount of data has evidenced the contribution of non-CYP metabolism to elimination of drug candidates. For instance, while introducing polar functional groups such as hydroxyl or carbonyl groups does indeed reduce lipophilicity of compounds, thereby proving useful in preventing CYP metabolism during lead optimization in drug discovery, these units are subsequently targeted by phase II metabolism such as conjugation (Nassar et al., 2004, Thompson, 2001). Indeed, the UDP-glucuronosyltransferase family contribute to clearance for approximately 10% of the top 200 drugs prescribed in the United States in 2002, and glucuronidation is the next major clearance mechanism for these drugs following CYP family (Williams et al., 2004). Likewise, flavin-containing monooxygenase and monoamineoxidase have significant contributions to clearance for some of the top 200 drugs (Williams et al., 2004). In addition, efforts to reduce CYP metabolic liability have led to development of a number of compounds that are instead cleared by aldehyde oxidase (AO) (Torres et al., 2007). Or Rosemond and Walsh (2004) reported that carbonyl reduction is the major or sole metabolic pathway for several clinical drugs, where carbonyl and aldo-keto reductase are major isoform contributing to

drug metabolism. However, given that AO and certain members of the reductase family are cytosolic enzymes, current microsome-based methods do not adequately and completely describe metabolic activities; indeed, several studies have reported the risk of underestimating AO metabolism in humans (Hutzler et al., 2012, Zientek et al., 2010).

Despite these situations, species differences in extra-hepatic or non-CYP metabolism remains un-clarified. Consequently, the methods of human pharmacokinetics prediction with respect to these metabolic pathway have not been sufficiently developed. As such, novel approaches to complement liver microsome-based prediction methods are needed to evaluate human extra-hepatic or non-CYP metabolic pathways.

Here, I examine the impacts of species differences in intestinal and AO metabolism on human pharmacokinetic prediction in the drug discovery process and assess a novel approach to predicting AO metabolism in humans.

1. A comparison of pharmacokinetics between humans and monkeys

1.1 Introduction

When predicting human pharmacokinetics, the Fa, Fg, and Fh are the main factors to consider. Fh prediction has become considerably accurate since several mathematical prediction models have been established, including the physiological model, well stirred model, parallel tube model, and dispersion model (Iwatsubo et al., 1996; Naritomi et al., 2001; De Buck et al., 2007). For FaFg, however, no quantitative prediction method has ever been established, although several qualitative prediction methods using human intestinal microsomes have been reported (Chiba et al., 1997; Shen et al., 1997; Fagerholm, 2007; Fisher and Labissiere, 2007; Yang et al., 2007). For these reasons, I have mainly used animal pharmacokinetic parameters to predict human FaFg in the drug discovery stage.

It has been regarded as natural that monkey metabolism is most similar to that of humans, so that cynomolgus monkeys have been widely used in pharmacokinetic or drug-safety studies for that reason. In the last decade, however, cynomolgus monkeys have often been found to have a poorer bioavailability (BA) than other animal species for many compounds (Tabata et al., 2009).

More recently, several reports have stated that the intestinal transit process, namely Fa or Fg, is a major contributor to the low BA in cynomolgus monkeys (Sakuda et al., 2006; Takahashi et al., 2008). However, unlike Fh, which can be easily calculated via conventional pharmacokinetic analysis, Fa and Fg are difficult to evaluate separately, particularly in the intestine. Consequently,

few systemic studies have explored the usefulness of monkey FaFg parameters to predict human pharmacokinetics.

Chiou and Buehler (2002) reported that the Fa and total clearance, corrected by hepatic blood flow rate, correlated well between humans and monkeys. This finding suggested that the species difference might be caused by Fg. In addition, it was also reported that midazolam (MDZ) had a markedly lower BA (2.0%) in cynomolgus monkeys than in humans (24–46%), which was caused by high first-pass intestinal metabolism (Sakuda et al., 2006). Similar results reported by Nishimura et al. (2007) showed that extensive metabolism in the intestine was the cause of MDZ's low BA in cynomolgus monkeys.

In this study, the following studies were performed to further investigate the species differences between humans and cynomolgus monkeys. Thirteen commercially available drugs for which the human pharmacokinetic parameters are known were selected and classified into five categories according to CYP isoform selectivity and P-gp affinity.

The 13 drugs were intravenously and orally administered to cynomolgus monkeys to obtain *in vivo* pharmacokinetic parameters (BA, Fh, and FaFg) for each drug, which were then compared with those in humans. In addition, I also obtained *in vitro* parameters for all 13 drugs, including protein binding, blood-to-plasma concentration ratio (Rb), membrane permeability, *in vitro* intrinsic clearance in liver microsomes ($CLint_{vitro,\ liver}$), $CLint_{vitro}$ in intestine microsomes ($CLint_{vitro,\ intestine}$), and P-gp affinity.

Here, I discuss the main factor affecting the species difference between humans and cynomolgus

monkeys indicated by these results. I also discuss the adequacy of cynomolgus monkeys as an animal model for predicting human pharmacokinetics.

1.2 Materials and Methods

1.2.1 Chemicals and reagents

MDZ (Dormicam, 5 mg/mL solution for intravenous injection) was obtained from Astellas Pharma Inc. (Tokyo). Tacrolimus (TAC) was synthesized at our laboratory. Lithium carbonate (Li) was purchased from Kanto Chemical Co., Inc. (Tokyo). Hydrochlorothiazide (HT), verapamil (VER), propranolol (PRO), and amitriptyline (AMI) were purchased from Wako Pure Chemicals (Osaka). Dexamethasone (DEX), nifedipine (NIF), quinidine (QID), timolol (TIM), and ibuprofen (IBU) were purchased from Sigma-Aldrich Corporation (St. Louis, MO, USA). Liver and intestine microsomes from humans and cynomolgus monkeys were purchased from XenoTech, LLC (Lenexa, KS, USA). All other reagents and solvents were commercial products of analytical grade.

1.2.2 Selected drugs and categorization

I allocated the 13 drugs into five categories (Type A–E), according to their pharmacokinetic properties in humans, as follows: membrane permeability, CYP isoform selectivity, and P-gp affinity (Yu, 1999; Kivisto et al., 2004; Yang et al., 2006) (Table 1-1).

Type A

The drugs categorized as Type A are indicator drugs that undergo no metabolism in humans and

are not P-gp substrates. For each of these, almost all of the absorbed drug is excreted into urine as the unchanged form. Li, which has a high BA in humans (94.5%) (Arancibia et al., 1986), and HT, which has a moderate BA in humans (60.2%) (Patel et al., 1984), were assigned to this category.

Type B

The drugs categorized as Type B are CYP3A4 substrates, and they have very weak, if any, affinity for P-gp. DEX, which has a high BA in humans (81.4%) (Duggan et al., 1975), NIF, and MDZ, which have a moderate BA in humans [41.2% (Holtbecker et al., 1996) and 30.0% (Thummel et al., 1996), respectively] were assigned to this category.

Type C

The drugs categorized as Type C are substrates of both CYP3A4 and P-gp. QID, which has a high BA in humans (79.5%) (Greenblatt et al., 1977), as well as TAC and VER, which have a moderate BA in humans [23.3% (Moller et al., 1999) and 18.0% (McAllister and Kirsten, 1982), respectively], were assigned to this category.

Type D

Digoxin (DIG), which is substrate of P-gp but not CYP3A4, was categorized as Type D. DIG has a high BA in humans (65.3%) (Hinderling and Hartmann, 1991) and undergoes almost no metabolism in the human body, i.e., it undergoes only P-gp efflux during the absorption process in the intestine.

Type E

The drugs categorized as Type E are mainly metabolized by the CYP isoform (except CYP3A4)

and have very weak, if any, affinity for P-gp. IBU and TIM, which have a high BA in humans [100% (Martin et al., 1990) and 61.0% (Wilson et al., 1982), respectively], as well as AMI and PRO, which have a moderate BA in humans [47.7% (Schulz et al., 1983) and 29.0% (Borgstrom et al., 1981), respectively], were assigned to this category. See Table 1-1 for CYP isoform that contribute to each drug metabolism.

Table 1-1;Classification of each drug based on CYP isoform selectivity and p-glycoprotein affinity

Type	Compounds	*BA* in Humans	P450 Isoform	P-gp Affinity	Reference
A	Lithium	94.5%	−	−	Arancibia et al., 1986
	Hydrochlorothiazide	60.2%	−	−	Patel et al., 1984
B	Dexamethasone	81.4%	3A4	±	Duggan et al., 1975
	Nifedipine	41.2%	3A4	−	Holtbecker et al., 1996
	Midazolam	30.0%	3A4	±	Thummel et al., 1996
C	Quinidine	79.5%	3A4	+	Greenblatt et al., 1977
	Tacrolimus	23.3%	3A4	+	Moller et al., 1999
	Verapamil	18.0%	3A4	+	McAllister and Kirsten, 1982
D	Digoxin	65.3%	−	+	Hinderling and Hartmann, 1991
E	Propranolol	29.0%	2D6, 1A2	−	Borgström et al., 1981
	Amitriptyline	47.7%	2C19, 2D6, 3A4	±	Schulz et al., 1983
	Timolol	61.0%	2D6	−	Wilson et al., 1982
	Ibuprofen	100.0%	2C9	−	Martin et al., 1990

1.2.3 Pharmacokinetic study in cynomolgus monkeys

Animals

Male cynomolgus monkeys (Shin Nippon Biomedical Laboratories, Ltd., Kagoshima, and Astellas Research Technology, Osaka) weighing approximately 5 kg were used. The animal experiment was conducted according to the ethical rules of each company.

Pharmacokinetic Study

Intravenous and oral administrations were performed with a washout period of at least 7 days between each type of administration. Animals were fasted for approximately 17 h before dosing. Blood samples were collected from the antebrachial vein, kept in an ice-water bath, and then centrifuged at 10,000 rpm for 1 min at 4°C. The plasma samples were kept in a deep freezer (approximately −20°C) until analysis. The experimental conditions for the pharmacokinetic studies, including doses, dosing solution, dosing volume, and sampling time for each drug, are shown in Table 1-2. Values obtained from the literature were used as the pharmacokinetic parameter values for all selected drugs in humans as well as those for MDZ in cynomolgus monkeys.

Table 1-2; Experimental conditions of cynomolgus monkey pharmacokinetic studies

Compounds	Dosing Route	Dose *mg/kg*	Vehicle	Volume *ml/kg*	Sample Points *h*
Lithium	Intravenous	5	Equivalent amount of hydrochloric acid	1	0.083, 0.25, 1, 3, 5, 8, 24
	Oral	10		2	0.25, 0.5, 1, 2, 4, 8, 24
Hydrochlorothiazide	Intravenous	1	50%PEG	1	0.25, 1, 1.5, 4, 6, 8, 24
	Oral	1		2	0.5, 1.5, 2.5, 4, 6, 8, 24
Dexamethasone	Intravenous	0.25	50%PEG	1	0.083, 0.25, 1, 2, 4, 6, 8
	Oral	0.5		2	0.25, 0.5, 1, 2, 4, 6, 8
Nifedipine	Intravenous	0.1	50%PEG	1	0.083, 0.25, 0.5, 1, 2, 4, 5
	Oral	1		2	0.25, 0.5, 1, 2, 4, 5
Midazolam (Sakuda et. al., 2006)	Intravenous	1	Distilled water [a]	1	0.1, 0.25, 0.5, 1, 2, 4, 8, 12, 24
	Oral	3		2	0.25, 0.5, 1, 2, 4, 8, 12, 24
Quinidine	Intravenous	1	Saline	1	0.1, 0.25, 0.5, 1, 2, 4, 8, 24
	Oral	3	Distilled water	2	0.25, 0.5, 1, 2, 4, 8, 24
Tacrolimus	Intravenous	0.004	Saline [b]	0.5	0.083, 0.25, 0.5, 1, 4, 8, 24
	Oral	0.02		2	0.25, 0.5, 1, 2, 4, 8, 24
Verapamil	Intravenous	1	Saline	1	0.1, 0.25, 0.5, 1, 2, 4, 8, 12, 24
	Oral	3		2	0.25, 0.5, 1, 2, 4, 8, 12, 24
Digoxin	Intravenous	0.1	50%PEG	1	0.1, 0.25, 0.5, 1, 2, 4, 8, 24
	Oral	0.1		2	0.25, 0.5, 1, 2, 4, 8, 24
Propranolol	Intravenous	0.3	Saline	2	0.1, 0.25, 0.5, 1, 2, 4, 8, 24
	Oral	1	Distilled water	2	0.25, 0.5, 1, 2, 4, 8, 24
Amitriptyline	Intravenous	0.3	Saline	2	0.1, 0.25, 0.5, 1, 2, 4, 8, 24
	Oral	1	Distilled water	2	0.25, 0.5, 1, 2, 4, 8, 24
Timolol	Intravenous	0.3	Saline	2	0.1, 0.25, 0.5, 1, 2, 4, 8, 24
	Oral	1	Distilled water	2	0.25, 0.5, 1, 2, 4, 8, 24
Ibuprofen	Intravenous	1	Saline	2	0.1, 0.25, 0.5, 1, 2, 4, 8, 24
	Oral	3	50%PEG	2	0.25, 0.5, 1, 2, 4, 8, 24

1.2.4 Measurement of model compounds plasma concentration in cynomolgus monkeys

The concentrations of model drugs in cynomolgus monkey plasma were determined by using atomic absorption, enzyme immunoassay analysis, or high-performance liquid chromatography (LC) coupled with tandem mass spectrometry (MS/MS) with sample pretreatment.

Atomic absorption method: Lithium

The lithium level in the plasma was determined by using atomic absorption in accordance with the method of Pybus and Bowers (1970).

Enzyme immunoassay analysis: Dexamethasone and tacrolimus

The DEX level in the plasma and the TAC level in the blood were determined by using enzyme immunoassay. After extraction (see below), an aliquot was used as the sample for analysis by enzyme immunoassay (Tamura et al., 1987).

A 50-μL aliquot of plasma was buffered with 1% skim milk/phosphate-buffered saline. After the addition of 1 mL of distilled water, the mixture was extracted with 5 mL of diethyl ether, and the solvent was removed under a stream of nitrogen gas. The residue was then dissolved in 250 μL of skim milk (1%)/phosphate-buffered saline.

LC-MS/MS analysis

The plasma concentrations of all other drugs were determined by using LC-MS/MS. The

LC-system comprised a LC-VP/LC-10A series (Shimadzu, Kyoto) or HP-1100 series high-performance liquid chromatography (HPLC: Agilent Technologies, Santa Clara, CA, USA). The MS/MS experiments were conducted by using API-2000 or API-3000 LC-MS/MS systems (AB SCIEX, Foster, CA, USA). The details of the LC-MS/MS conditions, including the machines and columns used for each drug, are shown in Table 1-3.

Hydrochlorothiazide

A 200-μL aliquot of plasma was buffered with 500 μL of phosphate buffer (10 mM) adjusted to pH 3.0. After adding 100 μL of acetonitrile and 20 μL of internal standard solution (1 μg/mL diclofenac in 50% acetonitrile), the mixture was extracted with 4 mL of ethyl acetate, and the solvent was removed under a stream of nitrogen gas. Then, the residue was dissolved in 100 μL of mobile phase, and a 40-μL aliquot was injected into the LC-MS/MS (molecular>product: *m/z* = 296 > 269 [M+H]−).

Nifedipine

A 50-μL aliquot of plasma, 50 μL of acetonitrile (50%), and 100 μL of internal standard solution (1 μg/mL of in-house compound A in acetonitrile) were mixed well and then centrifuged to remove precipitated protein. The supernatant (100 μL) was then decanted, and 30 μL was injected into the LC-MS/MS (molecular>product: *m/z* = 347 > 315 [M+H]+).

Quinidine, Verapamil, Propranolol, Amitriptyline, and Timolol

A 200-µL aliquot of plasma was buffered with 500 µL of saturated sodium bicarbonate solution. After the addition of 50 µL of acetonitrile and 50 µL of internal standard solution (1 µg/mL of in-house compound B in 50% acetonitrile), the mixture was extracted with 3 mL of tert-butyl methyl ether, after which the solvent was removed under a stream of nitrogen gas. The residue was then dissolved in 200 µL of mobile phase, and a 20-µL aliquot was injected into the LC-MS/MS (molecular>product: QID *m/z* = 325 > 307 [M+H]+, VER *m/z* = 455 > 165 [M+H]+, TIM *m/z* = 317 > 261 [M+H]+, AMI *m/z* = 278 > 117 [M+H]+, PRO *m/z* = 260 > 116 [M+H]+).

Digoxin

A 200-µL aliquot of plasma was buffered with 500 µL of phosphate buffer (10 mM) adjusted to pH 3.0. After the addition of 100 µL of acetonitrile and 50 µL of internal standard solution (1 µg/mL digitoxin in 50% acetonitrile), the mixture was extracted with 3 mL of ethyl acetate, and the solvent was removed under a stream of nitrogen gas. The residue was then dissolved in 100 µL of mobile phase, after which a 20-µL aliquot was injected into the LC-MS/MS (molecular>product: *m/z* = 798 > 391 [M+NH4]+).

Ibuprofen

A 200-µL aliquot of plasma was buffered with 500 µL of phosphoric acid (5 mM). After the addition of 50 µL of acetonitrile and 50 µL of internal standard solution (1 µg/mL of diclofenac in 50% acetonitrile), the mixture was extracted with 3 mL of tert-butyl methyl ether, and the solvent

was removed under a stream of nitrogen gas. The residue was then dissolved in 200 μL of mobile phase, and a 20-μL aliquot was injected into the LC-MS/MS (molecular>product: *m/z* = 205 > 161, [M+H]−).

Table 1-3; Apparatus and LC-MS/MS analytical conditions for each drug during the determination in cynomolgus monkey plasma.

Drug	Column	Column Temperature *°C*	Injection Volume *μL*	Flow Rate *ml/min*	Mobile Phase
Hydrochlorothiazide [a]	Inertsil ODS 3.3 μM (2.1 × 50 mm)	40	40	0.2	0.1% Formic acid: acetonitrile = 1:1
Nifedipine [a]	Inertsil ODS 3.5 μM (3.0 × 150 mm)	- [c]	30	0.2	Water: acetonitrile = 4:6
Quinidine [b]	Xterra MS C18 (4.6 × 50 mm)	40	10	0.3	20 mM Ammonium acetate (pH4.8): acetonitrile = 4:6
Verapamil [b]	Xterra MS C18 (4.6 × 50 mm)	40	10	0.3	20 mM Ammonium acetate (pH4.8): acetonitrile = 4:6
Digoxin [b]	Xterra MS C18 (4.6 × 30 mm)	40	20	0.3	2 mM Ammonium acetate: acetonitrile = 65:35
Propranolol [b]	Xterra MS C18 (4.6 × 50 mm)	40	10	0.3	20 mM Ammonium acetate (pH4.8): acetonitrile = 4:6
Amitriptyline [b]	Xterra MS C18 (4.6 × 50 mm)	40	10	0.3	20 mM Ammonium acetate (pH4.8): acetonitrile = 4:6
Timolol [b]	Xterra MS C18 (4.6 × 50 mm)	40	10	0.3	20 mM Ammonium acetate (pH4.8): acetonitrile = 4:6
Ibuprofen [b]	Xterra MS C18 (4.6 × 50 mm)	40	10	0.3	20 M Ammonium acetate (pH4.8): acetonitrile = 4:6

[a] HP1100 series HPLC and API-2000 MS/MS were used for hydrochlorothiazide and nifedipine.

[b] LC-VP/LC-10A series HPLC and API-3000 MS/MS were used for all other drugs.

[c] -;Room temperature.

1.2.5 *In vitro* parameters

Blood-to-plasma concentration ratio

One milliliter of human and cynomolgus monkey blood was spiked with 10 μL of standard solution (100 μg/mL; 1000 ng/mL final) and pre-incubated in a shaking water bath at 37°C for 10 min. A 200-μL aliquot was then analyzed to determine the drug concentration in the blood. The remaining samples were centrifuged at 1800g for 10 min at 4°C, after which the drug concentration in 200-μL aliquots of plasma was determined. The Rb was then calculated from the concentrations of drug per milliliter of blood and plasma. All data regarding TAC level in humans and cynomolgus monkeys were determined by blood level base because the Rb value of TAC has been reported to be nonlinear, with values between 10 and 40 depending on the drug concentration in humans (Wallemacq et al., 1993).

Parallel artificial membrane permeability assay

The parallel artificial membrane permeability assay (PAMPA) method was carried out by using a PAMPA Evolution instrument from pION INC. (Woburn, MA, USA) (Avdeef et al., 2005). The lipid solution consisted of a 20% (w/v) dodecane solution and lecithin mixture. The donor solutions consisted of test compounds dissolved in 10 mM dimethylsulfoxide diluted in pH 6.5 buffer (final concentration of 50 μM). The acceptor plate was filled with 1% (w/v) SDS in water, and the pH was adjusted to 7.4 with 1N hydrochloric acid. The test plate was incubated for 120 min at 30°C. The concentration of each test compound in the reference, donor, and acceptor plates was measured

with a UV plate reader. The permeability coefficient was calculated by using Evolution Library Manager software version 2.2 (pION INC.).

Plasma protein binding

The plasma protein binding (unbound drug fraction in plasma) was determined by using the equilibrium dialysis method or ultracentrifugation method and the following equations:

Protein binding (%) = (1-fp) × 100 (1-1)

fp = concentration in filtrate or supernatant/concentration in serum (1-1)'

where fp is the unbound drug fraction in plasma. The unbound drug fraction in blood (fb) was calculated by dividing fp by Rb.

Equilibrium dialysis method

A DIANORM dialysis device (Diachema, Zürich, Switzerland), which is impermeable to substances with molecular weights greater than 10,000, was used. Aliquots (3.5-mL) of human and cynomolgus monkey plasma were spiked with 35 μL of standard solution (100 μg/mL; 1000 ng/mL final) and pre-incubated in a 37°C shaking water bath for 10 min.

One milliliter of mixture and isotonic phosphate buffer solution (pH 7.4) was put into the dialyzing cell and receptor cell, respectively. After 4-h incubation at 37°C, the plasma mixture and buffer sample were stored in 100-μL aliquots at −20°C until analysis.

Ultracentrifugation method

Ten microliters of standard solution (100 μg/mL) was added to 1000 μL of human or cynomolgus monkey plasma. The calibration samples were prepared by adding 17 μL of acetonitrile (50%) to 1700 μL of human or cynomolgus monkey plasma. These samples were then centrifuged at 436,000g for 140 min at 37°C by using a Beckman Optimal TL ultracentrifuge (Beckman Coulter, Fullerton, CA, USA). After ultracentrifugation, the unbound fp was calculated by dividing the concentration of drugs in the supernatant by that in the plasma.

In vitro *metabolism in liver and intestine microsomes*

Metabolic study conditions

The time courses of the unchanged drugs were obtained. Each drug was incubated at 37°C with a reaction mixture (1 mL) containing 500 μL of potassium-phosphate buffer (200 mM; pH 7.4), 100 μL of 1 mM EDTA-NaOH (pH 7.4), 100 μL of liver or intestine microsomes solution (the final concentration of microsomal protein was 0.05 mg/mL for TAC, 0.5 mg/mL for HT and DIG, and 0.2 mg/mL for all other drugs), 190 μL of distilled water, and 10 μL of each compound solution in 50% acetonitrile (final concentration: 0.2 μM).

After a 5-min pre-incubation, the reaction was initiated by the addition of 100 μL of an NADPH-generating system. The reaction was terminated by adding 100 μL of reaction mixture to 200 μL of acetonitrile including the internal standard at various time periods. After stopping the

enzyme reaction, the reaction mixture of TAC and DIG was extracted with 3 mL of tertiary butyl methyl ether, and the solvent was removed under a stream of nitrogen gas. The residue was then dissolved in 150 μL of mobile phase, and a 10-μL aliquot was injected into the LC-MS/MS. The reaction mixture of DEX and NIF was centrifuged at 10,000g for 5 min. The supernatant (100 μL) was then decanted, and 30-μL aliquots were injected into the LC-MS/MS.

The reaction mixtures of all other drugs were centrifuged at 10,000g for 5 min. The supernatants (100 μL) were decanted, and 10-μL aliquots were injected into the LC-MS/MS.

LC-MS/MS conditions

In this experiment, the unchanged concentrations of all drugs were determined by using LC-MS/MS analysis. Mass number of molecular ion and product ion for each compounds were identified as follows (polarity, molecular>product): HT *m/z* = 296 > 269 [M+H]−; DEX *m/z* = 393 > 91 [M+H]+; NIF *m/z* = 347 > 315 [M+H]+; MDZ *m/z* = 326 > 291 [M+H]+; QID *m/z* = 325 > 307 [M+H]+; TAC *m/z* = 821 > 769 [M+NH4]+; VER *m/z* = 455 > 165 [M+H]+; DIG *m/z* = 780 > 85 [M+H]−; IBU *m/z* = 205 > 161 [M+H]−; TIM *m/z* = 317 > 261 [M+H]+; AMI *m/z* = 278 > 117 [M+H]+; PRO *m/z* = 260 > 116 [M+H]+.

The Prominence 2000 series (Shimadzu) was used as the LC-system. The MS/MS analyses were conducted on an API-3200 LC-MS/MS system (AB SCIEX). For TAC, an Alliance HT Waters 2790 separations module and Micromass Quattro Ultima (Waters Corporation, Milford, MA, USA) were used for the LC-MS/MS analysis.

The Supelco RP-Amide (3 μm, 3.0 × 31 mm; Supelco, Inc., Bellefonte, PA, USA) was used as the analysis column for HT and DIG. The Capcell PAK MG (3 μm, 2.0 × 35 mm; Shiseido Corporation, Kyoto) HPLC column was used for all other drugs.

The flow rate was 0.3 mL/min. The column temperature was 50°C. The gradient system was used, starting with an ammonium acetate concentration of 20 mM (pH 4.8)/acetonitrile (9:1) for 0.5 min, and increasing the ratio of acetonitrile to 20 mM ammonium acetate (pH 4.8)/acetonitrile (1:9) over 0.5 min, which was then held for 2.5 min. The initial conditions were restored over 0.1 min, after which the column was re-equilibrated for 1 min.

Calculation of CLint $_{\text{vitro}}$ *in liver microsomes*

CLint $_{vitro,\ liver}$ was calculated by using the following equation based on the time course of the residual ratio of the unchanged drugs as determined using least-squares linear regression (Naritomi et al., 2001):

$$\text{CLint}_{vitro,\ liver}\ (\text{mL/min/mg protein}) = \text{ke}/\text{microsomal protein concentration} \quad (1\text{-}2)$$

where ke is the disappearance rate constant.

In the case of liver microsomes study, the units of CLint $_{\text{liver}}$ values were converted to per kilogram of body weight by using the following equation:

$$\text{CLint}_{vitro,\ liver}\ (\text{mL/min/kg}) = \text{CLint}_{vitro,\ liver}\ (\text{mL/min/mg protein}) \times \text{SF1}\ (\text{mg protein/g liver}) \times \text{SF2}\ (\text{g liver/kg body weight}) \quad (1\text{-}3)$$

where SF1 is the microsomal protein content per gram of liver [48.8 was used for both species

(Naritomi et al., 2001), assuming that the SF1 in cynomolgus monkeys is the same as in humans] and SF2 is the liver weight per kilogram of body weight (25.7 and 30.0 were used for humans and cynomolgus monkeys, respectively) (Davies and Morris, 1993).

Calculation of CLint $_{\text{vitro}}$ *in intestine microsomes*

CLint $_{vitro,\ intestine}$ was calculated by using the following equation based on the time course of the residual ratio of the unchanged drugs as determined using least-squares linear regression (Naritomi et al., 2001):

CLint $_{vitro,\ intestine}$ (μL/min/mg protein) = ke/microsomal protein concentration (1-4)

P-gp ATPase assay

Each drug was dissolved in dimethylsulfoxide (0.1–100 μM final) and pre-incubated for 5 min with 2 μg/mL human P-gp membrane (BD Gentest, Woburn, MA, USA) in 50 mM MES buffer (pH 6.8 adjusted with Tris) containing 2 mM EGTA, 2 mM dithiothreitol, 50 mM potassium chloride, and 5 mM sodium azide. Then, the ATPase reaction was started by the addition of 50 mM Mg-ATP solution. After 20-min incubation at 37°C, the reaction was stopped by adding 20 μL of sodium dodecyl sulfate (10%) containing Antifoam A (Sigma-Aldrich Corporation). Subsequently, 200 μL of ammonium molybdate/zinc acetate was added for color development, and the mixture was incubated for another 20 min at 37°C. After incubation, the amount of liberated phosphate was measured by using the UV absorption method (630 nm). Baseline activity was determined by

reading incubated sodium orthovanadate (100 μM). Finally, ATPase activity was determined as the amount of liberated phosphate per milligram protein per minute. VER was evaluated in all ATPase assays, and the ATPase activity of each drug was normalized by dividing by the VER ATPase activity for each experiment.

1.2.6 Calculation of *in vivo* pharmacokinetic parameters

Plasma concentration data were analyzed individually at each point in time, and pharmacokinetic parameters were calculated by using a model-independent method. BA, FaFg, and Fh were then calculated from these pharmacokinetic parameters and Rb (see Blood-to-plasma concentration ratio under Materials and Methods) by using the formulas shown below. For Li and HT, I assumed that these drugs underwent almost no *in vivo* metabolism and that their FaFg values (meaning Fa in this case) were equal to BA. The BA values for the drugs in cynomolgus monkeys were determined by using the following equation:

$$BA\ (\%) = \{AUCinf\ (p.o.)/AUCinf\ (i.v.)\} \times (Dose\ i.v./Dose\ p.o.) \times 100 \qquad (1\text{-}5)$$

where AUCinf (i.v.) and AUCinf (p.o.) are the area under the plasma concentration-time curve calculated using the trapezoidal rule with extrapolation from the last measured plasma concentration to infinity after intravenous and oral administrations, respectively.

The Fh of drugs was determined by using the following equation and assuming that the elimination of drugs from the body after intravenous administration consisted of liver metabolism and renal excretion:

$$Fh = 1 - \{(CLh/Rb)/Qh\}, CLh = CLt \times (1 - fe) \quad (1\text{-}6)$$

where Qh is the blood flow rate in the liver (the human and cynomolgus monkey Qh values were 20.7 and 43.6 mL/min/kg, respectively) (Davies and Morris, 1993), CLh is hepatic clearance, CLt is total clearance, and fe is the urinary excretion ratio of the unchanged drug after intravenous administration. In cases where the fe value was not available, the CLh was assumed to be equal to the CLt.

The drug FaFg values were determined by using the following equations, assuming that the BA was expressed as the product of FaFg and Fh:

$$BA\ (\%) = Fa \times Fg \times Fh \times 100 \quad (1\text{-}7)$$

$$FaFg = \{BA\ (\%)/100\}/Fh. \quad (1\text{-}7)'$$

The BA, FaFg, and Fh values of each drug in humans were also calculated in a similar manner by using the reported pharmacokinetic parameters.

1.3 Results

1.3.1 Comparison of pharmacokinetic parameters between humans and monkeys

The *in vivo* pharmacokinetic parameters, BA, FaFg, and Fh, for all 13 drugs are summarized in Table 1-4. Each drug's cynomolgus monkey BA, FaFg, and Fh values are plotted against those in humans in Figure 1-1.

Correlation of the BA between Humans and Cynomolgus Monkeys

The BA values of all drugs observed in cynomolgus monkeys were compared with those in humans. The results showed that the BA value for Li, DEX, and IBU in humans and cynomolgus monkeys were similar, and that the BA value for HT and DIG were almost similar (<2-fold). In contrast, with the exception of DEX and IBU, many of the CYP substrate drugs had a markedly lower BA in cynomolgus monkeys than in humans.

Type A

The BA values for Li in humans and cynomolgus monkeys were similar (94.5%/97.9%), and HT showed slightly lower BA values in cynomolgus monkeys (30.7%) than in humans (60.2%).

Type B

For DEX, the BA values in humans and cynomolgus monkeys were similar (81.4 and 78.9%, respectively). However, the BA values for NIF and MDZ in cynomolgus monkeys were markedly lower [9.3 and 2.0% (Sakuda et al., 2006), respectively] than those in humans (41.2 and 30.0%, respectively).

Type C

The Type C drugs, QID, TAC and VER, which are known to be substrates for both CYP3A4 and P-gp in humans, had markedly lower BA values (4.5, 0.5, and 0%, respectively) in cynomolgus monkeys than in humans (79.5, 23.3, and 18.0%, respectively).

Type D

The DIG, which is a typical substrate of P-gp, had a slightly lower BA value in cynomolgus monkeys (45.0%) than in humans (65.3%). This finding was similar to that for HT.

Type E

Whereas the BA value of IBU was almost the same in both species, that for TIM, AMI, and PRO was lower in cynomolgus monkeys (10.8, 1.3, and 3.3%) than in humans (61.0, 47.7, and 29.0%). These findings were similar to those for Type B drugs. No significant correlation between the CYP isoform selectivity of drugs and their BA values in cynomolgus monkeys was observed.

Correlation of the Fh between humans and cynomolgus monkeys

The correlations between the human and cynomolgus monkey Fh values for the 13 drugs are shown in Figure 1-1B. The Fh values in cynomolgus monkeys were similar to those in humans for all drugs except VER (Fh was calculated as 0 in cynomolgus monkeys), because the plots for the drugs were the same or nearly the same (Fig. 1-1B; Table 1-4). Li and HT underwent almost no *in vivo* metabolism; therefore, the Fh values were considered to be 1.

Correlation of the FaFg between humans and cynomolgus monkeys

As shown in Figure 1-1C, the FaFg values for Li, DEX, and IBU were similar in both humans and

cynomolgus monkeys (0.95/0.98, 0.93/0.85, and 1/1, respectively). For HT and DIG, the FaFg values in cynomolgus monkeys were slightly lower than those in humans (0.60/0.31 and 0.67/0.48 in humans and cynomolgus monkeys, respectively).

For the other 7 drugs (except VER), the BA in cynomolgus monkeys was low, and a markedly low FaFg was observed. These tendencies correlated well with those of the BA values (assuming Fh = 1 for Li and HT, which means BA = FaFg).

A

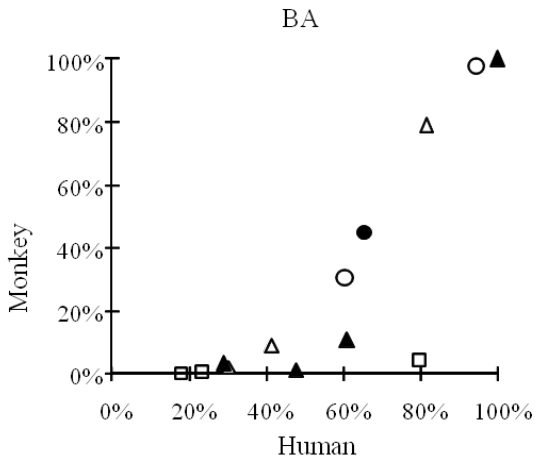

B

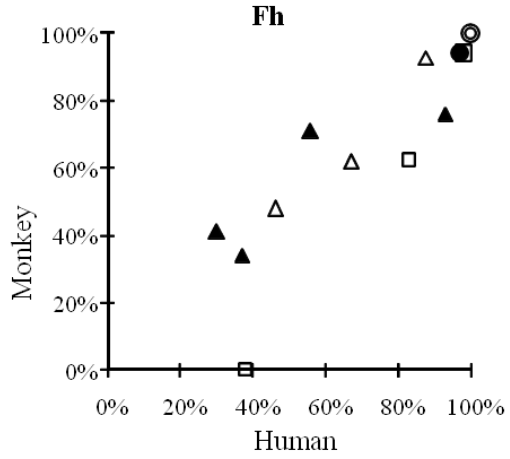

C

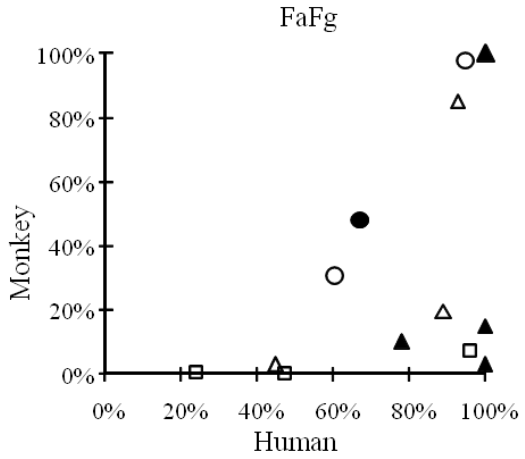

Figure 1-1. Correlation of BA (A), Fh (B), and FaFg (C) in humans and cynomolgus monkeys.

Open circle, open triangle, open square, closed circle, and closed triangle represent category Types A-E, respectively.

Table 1-4; Summary of *in vivo* pharmacokinetic parameters in humans and cynomolgus monkeys.

Drugs	Species	Dose (i.v./p.o.)	CLt	fe	CLh	BA	FaFg	Fh
		mg/kg	*mL/min/kg*	*%*	*mL/min/kg*	*%*		
Lithium	Human	(−/0.25)	0.4 ± 0.2	No data	0[a]	94.5 ± 15.8	0.95	1[a]
	Monkey	0.14/0.27	0.7 ± 0.1	No data	0[a]	97.9 ± 6.8	0.98	1[a]
Hydrochlorothiazide	Human	(−/0.32)	3.0 ± 1.0	60.2	0[a]	60.2	0.6	1[a]
	Monkey	1/1	5.9 ± 2.0	No data	0[a]	30.7 ± 9.4	0.31	1[a]
Dexamethasone	Human	0.17/0.17	2.7 ± 0.8	10.8 ± 4.3	2.4	81.4 ± 15.8	0.93	0.88
	Monkey	0.25/0.5	4.5 ± 0.8	No data	4.5	78.9 ± 9.8	0.85	0.93
Nifedipine	Human	0.02/0.27	8.2 ± 0.6	No data	8.2	41.2 ± 5.4	0.89	0.46
	Monkey	0.1/1	15.6 ± 3.5	0.057	15.6	9.3 ± 4.0	0.19	0.48
Midazolam	Human	0.013/0.026	4.7 ± 1.5	0.27 ± 0.07	4.7	30.0 ± 10.0	0.45	0.67
	Monkey	1/3	12.9 ± 1.8	<1%	12.9	2.0 ± 0.4	0.03	0.62
Quinidine	Human	4.3/5.0	3.8 ± 0.3	35.1 ± 1.8	2.5	79.5 ± 15.0	0.96	0.83
	Monkey	1/3	12.8 ± 0.7	0.6 ± 0.2	12.7	4.5 ± 1.7	0.07	0.62
Tacrolimus	Human	0.02/0.05	0.5 ± 0.1	0.04 ± 0.02	0.5	23.3 ± 16.7	0.24	0.98
	Monkey	0.004/0.02	2.6 ± 0.3	No data	2.6	0.5 ± 0.5	0.005	0.94
Verapamil	Human	0.14/1.14	11.8 ± 0.5	No data	11.8	18.0 ± 10.1	0.47	0.38
	Monkey	1/3	44.9 ± 10.5	1.5 ± 0.7	44.2	0	–[b]	0
Digoxin	Human	0.01/0.01	2.9 ± 0.6	80.5 ± 3.2	0.6	65.3 ± 22.5	0.67	0.97
	Monkey	0.1/0.1	2.9 ± 0.03	17.1 ± 9.3	2.4	45.0 ± 14.0	0.48	0.94
Propranolol	Human	0.13/0.5	11.6[c]	No data	11.6	29	0.78	0.37
	Monkey	0.3/1	24.3 ± 2.4	No data	24.3	3.3 ± 1.5	0.1	0.34
Amitriptyline	Human	0.6/1.2	12.5 ± 2.3	No data	12.5	47.7 ± 11.0	1[d]	0.3
	Monkey	0.3/1	35.8 ± 8.8	0.2 ± 0.2	35.7	1.3 ± 1.0	0.03	0.41
Timolol	Human	0.025/0.4	7.7 ± 3.7	No data	7.7	61.0 ± 19.2	1[d]	0.56
	Monkey	0.3/1	13.6 ± 0.4	4.8 ± 2.6	13	10.8 ± 4.3	0.15	0.71
Ibuprofen	Human	2.9/4.2	0.8 ± 0.2	No data	0.8	102.8 ± 12.0	1[d]	0.93
	Monkey	1/3	7.9 ± 0.7	18.5 ± 1.1	6.4	103.4 ± 14.2	1[d]	0.76

[a] Assuming CLh was 0, e.g., the Fh values were 1.

[b] Not calculated.

[c] CLt was calculated by dividing dose by AUC after intravenous administration.

[d] The calculated values were greater than 1.

1.3.2 *In vitro* parameters

In this study, some additional *in vitro* assays were performed to evaluate the drugs' (except Li) *in vitro* pharmacokinetic properties. These assays included determination of the Rb, membrane permeability, *in vitro* metabolic stability assay using human and cynomolgus monkey liver and intestine microsomes, plasma protein binding, and P-gp affinity. The results are summarized in Table 1-5.

Membrane permeability

As shown in Table 1-5, almost all drugs except HT and DIG showed good membrane permeability (apparent permeability coefficient of more than 10). Taking the BA values into consideration, the HT and DIG were speculated to be absorbed moderately in cynomolgus monkeys. These results suggest that all tested drugs were well absorbed or relatively well absorbed in cynomolgus monkeys, even though many drugs had a low BA.

Metabolic stability in liver microsomes

For HT and DIG, no depletion was observed, and the $CLint_{vitro,\ liver}$ for DEX MDZ, and IBU in both humans and cynomolgus monkeys were almost the same (66/24 mL/min/kg, 877/1422 mL/min/kg, and 38/25 mL/min/kg, respectively). $CLint_{vitro,\ liver}$ values for the other seven drugs were higher in cynomolgus monkeys than in humans (Table 1-5). Although Fh correlated well between humans and cynomolgus monkeys for all tested drugs except VER, these drugs were

metabolized more rapidly in cynomolgus monkey microsomes than in human microsomes. Furthermore, the fb × $CLint_{vitro, liver}$/Qh for NIF, VER, PRO, and AMI were found to be higher (>4) after taking fb and blood flow rate in the liver into consideration, indicating that these drugs might undergo rapid metabolism in the liver of cynomolgus monkeys.

Metabolic stability in intestine microsomes

The $CLint_{vitro, intestine}$ was expressed by μL/min/mg protein because there is no widely used physiological conversion model from μL/min/mg protein to μL/min/kg in intestine. The $CLint_{vitro, intestine}$ values for NIF, MDZ, QID, TAC, and VER in cynomolgus monkey intestine microsomes were 612, 1635, 212, 4663, and 696 μL/min/mg protein, respectively. As well as in human, the values were 138, 385, no depletion, 625, and 69 μL/min/mg protein for each (Fig. 1-2; Table 1-5). In contrast, no significant decreases in other drugs were observed in both human and cynomolgus monkey intestine microsomes.

ATPase assay

The ATPase activity of all drugs was normalized by dividing them by the VER value. As shown in Table 1-5, the ATPase activity of QID, DIG, and TAC was higher than that of VER. For PRO, AMI, TIM, and IBU, the ATPase activity values were similar to the VER value, whereas the HT, DEX, NIF, and MDZ were lower. No significant correlation between P-gp affinity and BA values in cynomolgus monkeys was observed.

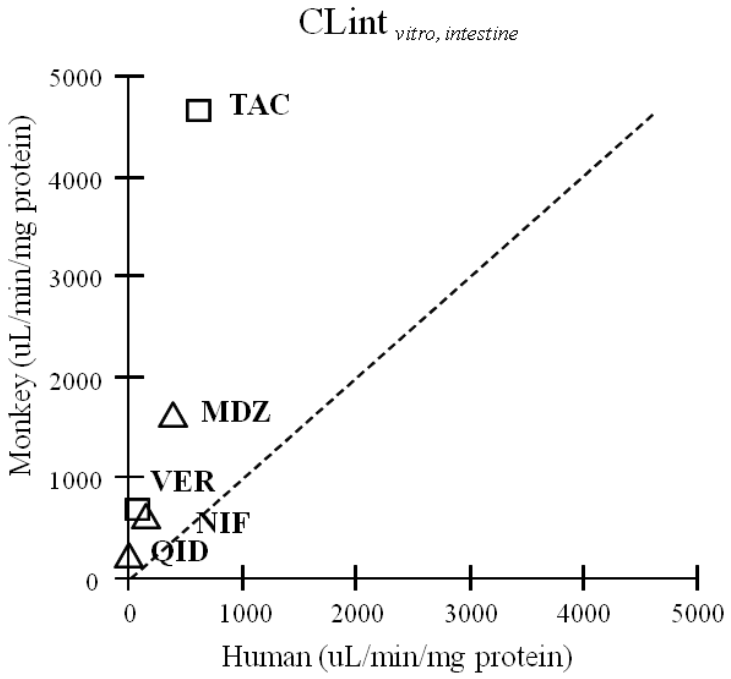

Figure 1-2. Correlation of CLint *vitro, intestine* in humans and cynomolgus monkeys.

NIF, MDZ, QID, TAC, and VER represent nifedipine, midazolam, quinidine, tacrolimus, and verapamil, respectively.

Table 1-5; Summary of *in vitro* pharmacokinetic parameters of tested drugs in humans and cynomolgus monkeys.

Drugs	Species	Rb	Papp	Protein binding	fp	fb	CLint *vitro, liver*	CLint *vitro intestine*	fb x CLint *vitro, liver*/Qh	ATPase *ratio vs VER*
			×10⁻⁶cm/s	%			*mL/min/kg*	*µL/min/mg protein*		
Hydrochlorothiazide	Human	2.7	0.1	40	0.6	0.222	–[a]	–[a]	–[a]	0
	Monkey	1.84		39	0.61	0.331	–[a]	–[a]	–[a]	NT
Dexamethasone	Human	0.95	16.4	52	0.48	0.507	66	–[a]	1.62	0.01
	Monkey	1.34		77.5	0.225	0.167	24	–[a]	0.09	NT
Nifedipine	Human	0.74	13.4	93.4	0.066	0.089	438	138	1.89	0.03
	Monkey	0.65		94.3	0.057	0.088	2597	612	4.96	NT
Midazolam	Human	0.69	30.8	97	0.03	0.044	877	385	1.85	0.28
	Monkey	0.77		95.7	0.043	0.056	1422	1635	1.72	NT
Quinidine	Human	0.72	17.9	91.4	0.086	0.119	52	–[a]	0.3	4.57
	Monkey	0.78		92.1	0.079	0.102	872	212	1.91	NT
Tacrolimus	Human	20	34.2	98.9	0.011	0.001	1538	625	0.04	7.89
	Monkey	20		99	0.01	0.001	5793	4663	0.06	NT
Verapamil	Human	0.92	35.8	95.2	0.048	0.052	656	69	1.65	1
	Monkey	0.93		88.2	0.118	0.127	2491	696	6.83	NT
Digoxin	Human	1	0.1	60.3	0.397	0.398	–[a]	–[a]	–[a]	56.1
	Monkey	0.82		52.9	0.471	0.574	–[a]	–[a]	–[a]	NT
Propranolol	Human	0.89[b]	37.4	86	0.14	0.157	165	–[a]	1.25	1.7
	Monkey	0.85[c]		78.8	0.212	0.249	974	–[a]	5.25	NT
Amitriptyline	Human	0.86[d]	53.3	85.4	0.146	0.17	80	–[a]	0.66	1.2
	Monkey	1.4		87.2	0.128	0.091	2559	–[a]	5.06	NT
Timolol	Human	0.84[b]	27.3	50.9	0.491	0.585	32	–[a]	0.89	1.66
	Monkey	1.02		95.5	0.045	0.044	391	–[a]	0.37	NT
Ibuprofen	Human	0.55[d]	29.4	98.8	0.012	0.022	38	–[a]	0.04	1.14
	Monkey	0.61		98.5	0.015	0.024	25	–[a]	0.01	NT

Lithium was excluded from all *in vitro* studies. Papp, apparent permeability; NT, not tested.

a The CLint could not be calculated because the tested drug was not depleted.

b Data were taken from Shibata et al., 2002.

c Data were taken from Evans et al., 1973.

d Data were taken from Obach RS 1999.

1.4 Discussion

Although cynomolgus monkeys are often used for pharmacokinetic studies for drug discovery, it remains unclear whether this is a useful animal species for predicting human pharmacokinetics. In this study, I investigated the pharmacokinetic profile of 13 commercially available drugs in cynomolgus monkeys and compared their pharmacokinetic parameters with those in humans. The results showed that the majority of the drugs tested (8 of 13) had a markedly lower BA in cynomolgus monkeys (<15%). I explored the reasons for these species differences and suggest some possibilities as listed below.

Species differences in hepatic metabolism

The Fh values in humans and cynomolgus monkeys were almost the same for the 12 drugs (except VER). No obvious species differences were revealed for hepatic metabolism, regardless of CYP isoform selectivity. These results suggested that the values obtained from cynomolgus monkeys after intravenous administration were useful for predicting human pharmacokinetic parameters, such as CLt or Fh. These findings agreed with the consistency seen between the species with regard to CYP isoform amino acid sequence (over 90% agreement) (Uno et al., 2007).

A species difference in Fh was apparent for VER, which was explained by the difference in the rate of hepatic metabolism. The $fb \times CLint_{vitro,\ liver}/Qh$ of VER in cynomolgus monkeys was much higher than that in humans, which agreed with the *in vivo* observation.

Species differences in the intestinal transit process

The fact that all drugs with a low BA in cynomolgus monkeys had low FaFg values indicates that the low FaFg is attributable to the low BA, in cynomolgus monkeys specifically. The FaFg values for Li, DEX, and IBU were correlated well between humans and cynomolgus monkeys. The common properties of these three drugs are as follows: 1) they have good membrane permeability (Li is absorbed via a paracellular pathway); 2) they are not P-gp substrates; and 3) they undergo little or no *in vivo* metabolism (see Tables 1-4 and 1-5).

Subsequently, the FaFg correlation between humans and cynomolgus monkeys was found to be weak for both HT and DIG. The FaFg values for these drugs in cynomolgus monkeys were slightly lower than those in humans. The common properties of these two drugs are as follows: 1) they have moderate membrane permeability, and 2) they undergo almost no *in vivo* metabolism (Tables 1-4 and 1-5). Although HT is not a P-gp substrate, DIG was found to cause high activity in the ATPase assay. These results suggest that membrane permeability and P-gp efflux are partial contributors to the low BA in cynomolgus monkeys.

In contrast, the other seven drugs (except VER), which had a markedly low FaFg in cynomolgus monkeys, were metabolized by CYP enzymes and had relatively high $CLint_{vitro}$ values in cynomolgus monkeys liver or intestine microsomes. These drugs also showed good membrane permeability (Table 1-5).

These findings suggest the possibility that these drugs are extensively metabolized in the cynomolgus monkey intestine, and the low FaFg is caused by intestinal metabolism rather than

poor absorption. In fact, all of five drugs, which observed good FaFg correlation in both species, undergo little or no *in vivo* CYP metabolism.

The major species difference factor between humans and cynomolgus monkeys

There have been several reports that focused on the species differences between humans and monkeys (Chiou et al., 2002; Sakuda et al., 2006; Takahashi et al., 2008). However, the present study showed that drugs that satisfy the following properties have similar FaFg or BA values in both humans and cynomolgus monkeys: 1) good membrane permeability; 2) not a P-gp substrate; and 3) undergoes little or no *in vivo* metabolism.

In contrast, drugs that are CYP substrates and are relatively or rapidly metabolized in cynomolgus monkeys could have markedly low BA values because of their low FaFg values, even if the drugs have a low CLt. The potential reasons for these findings are as follows: 1) the amount of CYP enzyme expressed in cynomolgus monkey intestine is higher than that in humans, even though CYP3A4 is a major intestinal enzyme in humans; and 2) the enzyme expressed in cynomolgus monkey intestine has higher activity (Vmax/Km) than that in humans. To clearly understand these speculations, additional *in vitro* studies using intestine microsome were conducted with the same condition as the liver microsomes study. In cynomolgus monkey, the values of $CLint_{vitro,\ intestine}$ for NIF, MDZ, QID, TAC, and VER were 612, 1635, 212, 4663, and 696 μL/min/mg protein, respectively. As well as in human, the values were 138, 385, no depletion, 625, and 69 μL/min/mg protein for each. These five compounds, which have low BA in cynomolgus monkey, showed

markedly larger values in cynomolgus monkey than those in human (Fig. 1-2). In contrast, no significant decreases in other drugs were observed in both human and cynomolgus monkey intestine microsomes.

Whereas the cynomolgus monkey CYP isoform corresponding to human CYP3A4 is CYP3A8 (Uno et al., 2007), it is unclear whether CYP3A8 is also a major enzyme in the cynomolgus monkey intestine. In fact, a lower FaFg in cynomolgus monkeys was also observed for Type E drugs (mainly metabolized by CYP 2C9, 2C19, or 2D6 in humans).

Although it is possible that glucuronide conjugates contributed to the low BA obtained for PRO (Walle et al., 1979), further studies are needed to explain this observation. Because all drugs with a low BA in cynomolgus monkeys show good membrane permeability in the present study, first-pass intestinal metabolism must be the most critical factor affecting species differences between humans and cynomolgus monkeys.

I also investigated the pharmacokinetics of several drugs in rats and/or dogs, and the FaFg in rats or dogs correlates better with humans than cynomolgus monkeys (Tabata et al., 2009). Further studies are needed to clarify the species differences for FaFg, including the contribution of permeability, intestinal first-pass metabolism, and P-gp excretion.

The usability of cynomolgus monkey pharmacokinetic parameters for predicting pharmacokinetic in humans

These results suggest that a go/no go decision does not have to be made immediately, even if a

candidate has a markedly low BA in cynomolgus monkeys. In such cases, the main factor causing low BA in cynomolgus monkeys may be evaluated separately from Fa, Fg, and Fh. If the cause is found to be Fg, the candidate could still have an acceptable pharmacokinetic profile in humans.

Since recognition of the importance of intestinal metabolism has increased over recent years, many studies using intestinal microsomes may be in progress in an attempt to establish a system for evaluating human Fg.

It is noteworthy that a rough correlation was observed between $CLint_{vitro,\ liver}$ and Fg in humans (Fig. 1-3) in this study, indicating the possibility that Fg prediction in humans using only *in vitro* parameters may be possible with slight but elaborated modification of the evaluation system for *in vitro* intestinal metabolism. In fact, when evaluation of intestinal metabolism was inadequate, I successfully predicted the human pharmacokinetics for several in-house candidate drugs with a markedly low BA in cynomolgus monkeys by using human *in vitro* parameters for each candidate, including membrane permeability, metabolic stability in liver microsomes, and P-gp affinity (in-house data). These low values for BA in cynomolgus monkeys were virtually thought to be due to low Fg.

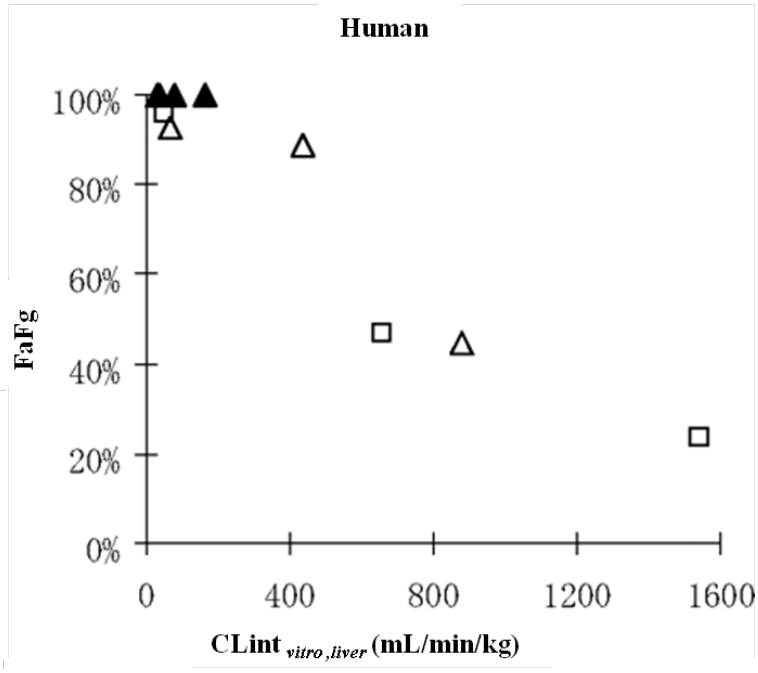

Figure 1-3. Correlation of FaFg and CLint $_{vitro,\ liver}$ in humans.

Open triangle, open square, and closed triangle represent category Types B, C, and E, respectively.

In conclusion, many drugs had a markedly low BA in cynomolgus monkeys despite having relatively good BA in humans. These findings are speculated to be attributable mainly to first-pass intestinal metabolism. Consequently, the pharmacokinetic parameters obtained for a candidate after oral administration to cynomolgus monkeys are not adequate for directly predicting human pharmacokinetics.

The accurate prediction of Fg in humans eventually becomes necessary to predict human pharmacokinetics with more accuracy. In addition, the slight but elaborated modification of the evaluation system for *in vitro* intestinal metabolism such as simplified intestinal availability model (Kadono et al., 2010), may enable us to estimate the Fg in humans, and subsequently it becomes possible to predict accurate human pharmacokinetics in the near future.

2. Extensive metabolism of FK3453 by aldehyde oxidase in humans

2.1 Introduction

Predicting human pharmacokinetics of drug candidates at the discovery stage of drug development is crucial to prevent candidate attrition in a phase 1 study. In particular, CYPs have been recognized as the most important drug metabolizing enzymes in regulating exposure of drugs administered orally. Indeed, a phase 1 study found that poor exposure of drug candidates was the most significant cause of candidate attrition, accounting for approximately 40% of all candidate loss in the early 1990s (Kola and Landis, 2004). Given its significant influence on ensuring compound promotion, a considerable number of studies have been focused on predicting CYP metabolism in humans over the past few decades (De Buck et al., 2007; Iwatsubo et al., 1996; Naritomi et al., 2001). Subsequently, several techniques have been developed to predict human pharmacokinetics, thereby helping to reduce the rate of attrition due to poor BA in the clinical stage (Wishart, 2007). In addition, screening systems to evaluate candidate compounds' CYP metabolic stability have also been developed, facilitating selection of those compounds most stable against CYP metabolism.

Increased attention has also been focused on the role of non-CYP enzymes in elimination of drug candidates from the body. Given that most existing methods of predicting human pharmacokinetics were established based solely on CYP metabolism, great care must be taken with regard to predicting pharmacokinetics for those candidates primarily metabolized by non-CYP

enzymes. FK3453 [6-(2-amino-4-phenylpyrimidin-5-yl)-2-isopropylpyridazin-3(2H)-one] (Fig. 2-1), a novel adenosine A1/2 dual inhibitor for the treatment of Parkinson's disease (Mihara et al., 2007, 2008a, b), is one such example of an in-house clinical drug candidate which undergoes extremely little metabolism by CYPs in humans *in vitro*. Although the preclinical pharmacokinetic profiles suggested favorable pharmacokinetics of FK3453 in humans, compound development was suspended due to extremely low plasma concentrations of unchanged drug in a phase 1 study. Underestimation of the contribution of non-CYP metabolism resulted in our inaccurately predicting the human pharmacokinetics of FK3453, subsequently resulting in these unexpected findings (described as below).

Here, to address the difficulty of predicting human pharmacokinetics for non-CYP metabolism, I describe a series of pharmacokinetic studies for development of FK3453 from preclinical to clinical stages. I also include pharmacokinetics findings for FK3453 after intravenous and oral administration to rats and dogs and oral administration to humans, as well as *in vitro* pharmacokinetic profiles. In addition, I also discuss the mechanism behind the low systemic exposure of FK3453 in humans.

2.2 Materials and Methods

2.2.1 Chemicals and reagents

FK3453 and its oxidative metabolite of the aminopyrimidine moiety (M4) synthesized at our laboratory were used (Fig. 2-1). [^{3}H]-FK3453 (specific radio activity: 38.9Ci/mmol, radioactive

purity: >98.6%) was synthesized by GE Healthcare Japan (Tokyo). Liver microsomes from rats and dogs were purchased from Celsis In Vitro Technologies (Baltimore, MD, USA), and liver microsomes and S9 from humans were purchased from XenoTech LLC. Allopurinol, 1-aminobenzotriazole, and menadione were purchased from Sigma-Aldrich Corporation. Isovanillin was purchased from ICN Biomedical Inc. (Aurora, OH, USA). All other reagents and solvents were commercial products of analytical grade.

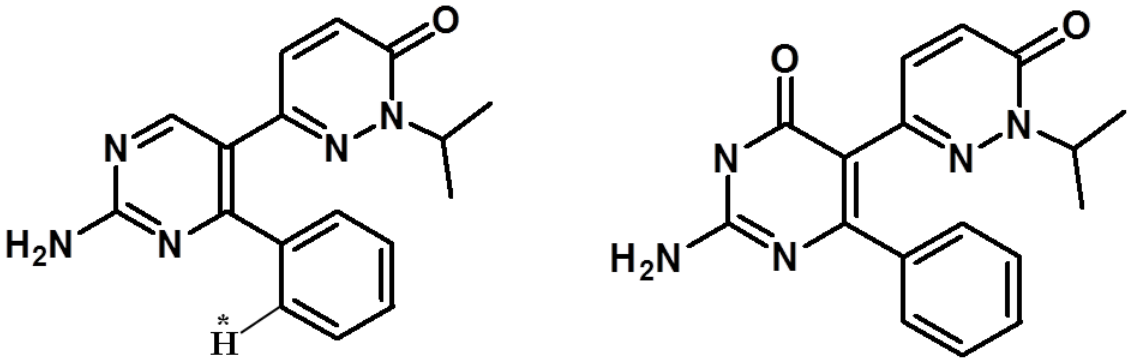

FK3453 M4

Figure 2-1. Chemical structures of FK3453 and M4 (*:^{3}H).

2.2.2 Pharmacokinetic study in humans

Design

This was a Phase I, double-blind, placebo-controlled single ascending dose, sequential group study. The primary objective was to evaluate the safety, tolerability and Pharmacokinetics of FK3453. It was planned to study a total of 72 subjects, in nine groups of eight (Groups A to I).

However, following completion of the third group of eight subjects (Group C), the study was terminated due to plasma levels of parent compound being markedly lower than anticipated.

Subjects and dosing

A total of 24 healthy male subjects aged between 21 and 41 years and weighing between 58 and 92 kg were enrolled into the study. The protocol was approved by an institutional review committee before study initiation, and all subjects gave their written informed consent to participate before starting. The subjects were assigned to Groups A, B, and C (n=6 active and 2 placebo). A single dose of FK3453 was administered orally at a dose of 0.5, 1, and 10 mg, respectively. Blood samples were taken by venipuncture or cannulation of a forearm vein. Samples were collected into 10 mL lithium heparin Vacutainer tubes at 0 (before dosing), 15, and 30 min, and 1, 1.5, 2, 3, 4, 6, 8, 10, 12, 24, 48, 72, and 96 h after administration. All plasma samples were stored at -20 °C until analysis.

2.2.3 Pharmacokinetic study in animals

All animal procedures described below were conducted according to the animal ethics rules at each facility involved in the study.

Rats

Male and female Sprague-Dawley rats were purchased from Charles River Japan Inc. (Tokyo). Rats weighing 200-250 g were fasted overnight before administration of dosing solution. FK3453

solution prepared with 100% PEG was administrated intravenously (0.1, 0.32, or 3.2 mg/kg) and orally (0.1, 0.32, or 3.2 mg/kg) to male rats and intravenously (0.1 or 1 mg/kg) and orally (0.32 or 1 mg/kg) to female rats. Blood samples were then collected from the inferior vein at predetermined times and stored at -20 °C until analysis.

Dogs

Three male beagle dogs weighing 10-15 kg were obtained from Ichiyanagi Farm (Shizuoka) and fasted overnight before administration of dosing solution. FK3453 solution prepared with 0.1N hydrochloric acid was administrated intravenously (0.1 mg/kg) and orally (0.03, 0.1, or 0.3 mg/kg) with a washout period of at least 7 days. Blood samples were then collected from the antecubital vein at predetermined times and stored at -20 °C until analysis.

2.2.4 Measurement of plasma concentration

Plasma samples were analyzed for presence of FK3453 (rats, dogs, and humans) and M4 (humans) using validated HPLC with LC-MS/MS.

Humans

A 1-mL aliquot of each human plasma sample was treated with 25 µL of internal standard solution prepared with 50% acetonitrile. After adding 1 mL of purified water, samples were applied to the solid-phase extraction column (Bond Elut C18, 200 mg/3 mL; VARIAN, Inc., Palo Alto, CA,

USA) pre-conditioned with methanol (3 mL) followed by purified water (3 mL). The column was then washed with 3 mL of water and eluted with 3 mL of methanol. After mixing the eluent, the organic solvent was evaporated under a stream of nitrogen gas, and the residue was subsequently dissolved in 500 μL of a mixture of water and methanol (70:30, v/v). The reconstituted solution was then passed through a membrane filter, and the resulting filtrate was used as the injection sample for analysis by LC (NANOSPACE SI-2, Shiseido Corporation)-MS/MS (TSQ Quantum; Thermo Fisher Scientific Inc., Waltham, MA, USA). A TSG-gel ODS-80Ts (5 μm, 2.0 mm ID x 150 mm; TOSOH, Tokyo) was used as the analysis column, and 5 mmol/L ammonium acetate and methanol (40:60, v/v) was used as the mobile phase. The substances were ionized by electro-spray ionization and detected in a positive mode using *m/z* 308>266 [M+H]+ for FK3453 and *m/z* 324>282 [M+H]+ for M4. The qualification limit was 0.025 ng/mL.

Rats and dogs

A 250-μL aliquot of each rat or dog plasma sample was treated with 25 μL of internal standard solution prepared with 50% acetonitrile. After adding 500 μL of 20 mmol/L sodium hydroxide solution and 5 mL of diethyl ether, samples were shaken for 10 min and centrifuged at 3000 rpm for 5 min. The organic layer (4.5 mL) was then transferred to glass tube, and the organic solvent was evaporated under a stream of nitrogen gas. The resulting residue was dissolved in 150 μL of mixture of water and acetonitrile (70:30, v/v), and 20-μL aliquots were analyzed by LC-MS/MS as described above. The qualification limit was 0.2 ng/mL.

2.2.5 *In vitro* parameters

Plasma protein binding

Plasma protein binding was determined via ultra filtration using the following equation:

plasma protein binding (%) = (1-unbound fraction in plasma [fp]) × 100 (2-1)

fp = concentrations in filtrate/concentrations in plasma (2-2)

Aliquots (4.5 mL) of male rat, dog, and human plasma were spiked with 22.5 μL of [^{3}H]-FK3453 standard solution (final concentrations: 2, 20, and 200 ng/mL, respectively) and pre-incubated for 5 min at 37 °C. One-millilitre aliquots of samples were then transferred to reservoirs of individual Centrifree® tubes (Millipore Co., Bedford, MA, USA) and centrifuged at 1500 g at 37 °C. To obtain an ultrafiltrate volume below 200 μL, centrifugation was set a 8 min for rat, 10 min for dog, and 12 min for human plasma samples. After centrifugation, the ultrafiltrate was transferred to a micro-test tube. Preliminary experiments showed that [^{3}H]-FK3453 was not adsorbed on the ultrafiltration device or membrane.

Before ultrafiltration, 1 mL of Soluene-350® (Packard Instrument Co., Meriden, CT, USA) was added to 25 μL of plasma solution to dissolve the biological specimens, and radioactivity was then measured by adding 10 mL of Econofluor-2® (Packard Instrument Co.). To measure radioactivity in the ultrafiltrate, 10 mL of Hionic-fluor® was added to 100 μL of the ultrafiltrate, and radioactivity was measured for 5 min using a liquid scintillation analyzer (2300TR; Packard Instrument Co.).

Blood to plasma concentration ratio

The Rb was calculated by dividing the concentrations of FK3453 in whole blood by that in plasma. Aliquots (4.5 mL) of male rat, dog, and human plasma were spiked with 22.5 μL of [^{3}H]-FK3453 standard solution (final concentrations: 2, 20, and 200 ng/mL, respectively) and pre-incubated for 5 min at 37 °C. After incubation, samples were divided into 2 tubes; one was used for blood concentration measurement, while the other was centrifuged at 3000 g for 1 min to separate the plasma fraction and then used for plasma concentration measurement. Both whole blood and plasma samples were measured for concentrations of radioactivity under similar conditions as those described above.

In vitro metabolic stability in liver microsomes

To determine the time course of the unchanged drug, FK3453 was incubated at 37 °C with a reaction mixture (500 μL) containing 250 μL of 200 mM potassium-phosphate buffer (pH 7.4), 50 μL of 1 mM EDTA-NaOH (pH 7.4), 25 μL of liver microsomes solution (final concentration of microsomal protein: 1 mg/mL), 170 μL of distilled water, and 5 μL of FK3453 solution in 50% acetonitrile (final concentration: 0.1 μmol/L). After 5 min of pre-incubation, the reaction was initiated by the addition of 50 μL of a NADPH-generating system and then terminated by adding 50 μL of reaction mixture to 200 μL of acetonitrile including the internal standard at 30, 60, and 120 min after incubation.

After stopping the enzyme reaction, the reaction mixture was centrifuged at 3000 g for 5 min at

4 °C. After adding 5 mL of acetonitrile to the supernatant, the solvent was evaporated under a stream of nitrogen gas, and the residue was dissolved in 250 µL of mobile phase consisting of 1 mmol/L perchloric acid solution and acetonitrile (90:10, v/v). Following this, a 20-µL aliquot was injected into the LC (LC-VP/LC-10A series; Shimadzu)-MS/MS (TSQ7000; Thermo Fisher Scientific Inc.) apparatus. The substances were ionized by electro-spray ionization and detected in a positive mode using *m/z* 308>266 [M+H]+ for FK3453. A CAPCELL PAK UG120 (3 µm, 4.6 mm ID × 150 mm; Shiseido Corporation) was used as the analysis column under the following gradient conditions: Gradient elution increased the ratio of 1 mmol/L perchloric acid and acetonitrile to 80:20 (v/v) over 15 min, 60:40 (v/v) over 15 min, and 50:50 (v/v) over 5 min, which was then held for a further 5 min. Initial conditions were restored over 1 min, after which the column was re-equilibrated for 9 min. The flow rate was 1.0 mL/min.

The $CLint_{vitro,\ liver}$ was calculated using the equations below and was based on the time-course of the residual ratio of the unchanged drugs, as determined using least squares linear regression (Naritomi et al., 2001).

$CLint_{vitro,\ liver}$ (mL /min/mg protein) = ke / microsomal protein concentration (2-3)

$CLint_{vitro,\ liver}$ (mL/min/kg) = $CLint_{vitro,\ liver}$ (mL/min/mg protein) × SF1 (mg protein/g liver) × SF2 (g liver/kg body weight) (2-4)

where ke is the disappearance rate constant (assumed to follow first-order kinetics), SF1 is the microsomal protein content per gram of liver (44.8, 77.9, and 48.8 for rats, dogs, and humans, respectively), and SF2 is the liver weight per kilogram of body weight (40.0, 32.0. and 25.7 for rats,

dogs, and humans, respectively) (Naritomi et al., 2001).

2.2.6 Calculation of *in vivo* pharmacokinetic parameters

Pharmacokinetic parameters were calculated via the model-independent method. Cmax and Tmax were determined from the mean of the actual values, and the AUCinf was calculated from the time-course change in concentrations of unchanged drug in plasma, based on the trapezoidal rule with extrapolation from the last measured plasma concentrations to infinity. CLt, half-life at the elimination phase (t1/2β), and volume of distribution (Vdss) were calculated using the following equations:

$$CLt = \text{Dose} / \text{AUCinf after intravenous administration} \quad (2\text{-}5)$$

$$t1/2\beta = \ln 2 / \lambda \quad (2\text{-}6)$$

$$Vdss = CLt \times AUMCinf / AUCinf \quad (2\text{-}7)$$

where λ is the slope of the final elimination phase estimated from the linear portion of the plasma concentration-time curve on a semi-logarithmic scale using the linear least squares method and AUMCinf is the area under the first order moment of plasma concentration-time curve extrapolated to infinity. BA was calculated from the ratio of the AUCinf values between intravenous and oral administration studies.

2.2.7 Prediction of human hepatic availability from *in vitro-in vivo* scaling

I predicted human Fh of FK3453 using the *in vitro-in vivo* scaling method, which involved

comparing $CLint_{vitro,\ liver}$ with $CLint_{vivo}$ in rats and dogs. The $CLint_{vivo}$ was calculated using the following equations, based on dispersion model (Iwatsubo et al., 1996):

$CLh = Qh \times (1-Fh)$ (2-8)

$Fh=4a / (1+a)2 \exp [(a-1)/2D_N] - (1-a)2 \exp [-(a+1)/2D_N]$ (2-9)

$a= [1+(4 \times fp/Rb \times CLint_{vivo} \times DN /Qh)]1/2$ (2-10)

where CLh is the hepatic clearance (assumed to be equal to CLt because urinary excretion of unchanged drug was negligible in rats and humans [data not shown]), Qh is hepatic blood flow rate (55.2, 30.9, and 20.7 mL/min/kg or rats, dogs, and humans, respectively) (Davis and Morris, 1993), and D_N is dispersion number (0.17 used for all calculations).

Human $CLint_{vivo}$ was predicted based on human $CLint_{vitro,\ liver}$ with a scaling factor, as follows:

Predicted human $CLint_{vivo}$ = human $CLint_{vitro,\ liver}$ × rat or dog scaling factor (2-11)

Scaling factor = $CLint_{vivo}$ / $CLint_{vitro,\ liver}$ (2-12)

2.2.8 *In vitro* metabolite profiling of FK3453 with human sub-cellular hepatic fractions

To determine the mechanism responsible for FK3453 metabolism, I conducted *in vitro* metabolite profiling using radio-chromatography analysis. [^{3}H]-FK3453 (final concentration: 0.1 μmol/L) was incubated with an NADPH-regenerating system and either human liver microsomes (1 mg/mL) or S9 (1 mg/mL) in a total volume of 1 mL of pH 7.4 phosphate buffer. Reactions were initiated by adding microsomes or S9 and then shaking the mixture in a water bath at 37 °C for 60 min. Reactions were terminated by adding 1 mL of acetonitrile and centrifuging the vial at 3000 g for 5

min at 4 °C. After evaporating the supernatant under a stream of nitrogen gas, the resulting residue was dissolved in 200 μL of mobile phase (1 mmol/L perchloric acid solution and acetonitrile, 90:10 [v/v]).

The samples were then subjected to radio-HPLC analysis, using a CAPCELL PAK UG120 (3 μm, 4.6 mm ID × 150 mm; Shiseido Corporation) as the analysis column. For the reaction mixture with microsomes, the gradient system described above was used. For the reaction mixture with S9, the gradient started with 1 mmol/L perchloric acid solution and acetonitrile at 90:10 (v/v) for 5 min, with the ratio increasing to 80:20 v/v over 15 min, 60:40 (v/v) over 15 min, and 20:80 (v/v) over 5 min, which was then held for 5 min. The initial conditions were restored over 1 min, after which the column was re-equilibrated for 9 min. A FLO-ONE/β A525AX device (PerkinElmer, Turku, Finland) was used to measure radioactivity.

For the inhibition study, 1-aminobenzotriazole (Ortiz de Montellano and Mathews, 1981; Mugford et al., 1992), menadione (Johns, 1967) and allopurinol (Massey et al., 1970), as inhibitors of CYPs, AO and xanthine oxidase (XO), respectively, were added to human liver S9 incubation mixtures at respective concentrations of 1000, 200, and 200 μmol/L.

Structural elucidation of metabolites for human liver microsomes and S9 was conducted using LC-MS and MS/MS systems. The LC-MS system consisted of a Waters model 717 plus auto-sampler, a Waters model 600s system controller, a Waters model 616 pump (Waters Corporation) and a TSQ7000 triple quadrupole mass spectrometer (Thermo Fisher Scientific Inc.). The reaction mixture after incubation was applied to the solid-phase extraction column (Bond Elut

C18, 200 mg/3 mL; VARIAN, Inc.) pre-conditioned with acetonitrile (3 mL) followed by purified water (3 mL) in that order. The column was then washed with 3 mL of water and eluted with 3 mL of acetonitrile. The eluent were mixed, and the organic solvent was evaporated under a stream of nitrogen gas. The resulting residue was then dissolved in 200 μL of mobile phase consisting of 5 mmol/L ammonium formate and acetonitrile (81.5:18.5, v/v), after which the samples were subjected to LC-MS and LC-MS/MS analysis. The gradient elution increased linearly from 18.5% B to 54.5% B over 20 min and was held at 54.5% B for 5 min before returning to 18.5%. The flow rate was 0.2 mL/min.

The identity of the metabolites was determined by confirming the mass fragmentation and chromatographic retention times to be identical to those of the reference compound and subsequently estimating the chemical structures of these metabolites and their metabolic pathways.

2.2.9 *In vitro* metabolic inhibition study of FK3453 with liver cytosol

To clarify the AO contribution to the FK3453 elimination in humans and animals, I conducted *in vitro* metabolic study using liver cytosol. FK3453 was incubated at 37 °C with a reaction mixture (500 μL) containing 250 μL of 200 mM potassium-phosphate buffer (pH 7.4), 50 μL of 1 mM EDTA-NaOH (pH 7.4), 100 μL of liver cytosol solution (final concentration of microsomal protein: 1 mg/mL for male and female rats, 2 mg/mL for dogs and humans, respectively), and 100 μL of distilled water. After 5 min of pre-incubation, the reaction was initiated by the addition of 5 μL of FK3453 solution in 50% acetonitrile (final concentration: 1 μmol/L) and then terminated by adding

100 μL of reaction mixture to 200 μL of acetonitrile including the internal standard at 15, 30, and 45 min after incubation.

After stopping the enzyme reaction, the reaction mixture was centrifuged at 3000 g for 5 min at 4 °C. 200 μL of the supernatant was injected into the glass vials. Following this, a 60-μL aliquot was injected into the LC apparatus (Alliance, Waters Corporation) -UV (2470 dual wavelength UV detector, Waters Corporation). A Inertsil ODS-3 (5 μm, 4.6 mm ID × 150 mm; GL Sciences Inc, Tokyo) was used as the analysis column with mobile phase of 200 mM potassium-phosphate buffer (pH 7.4) and acetonitrile to 60:40 (v/v). The flow rate was 1.0 mL/min.

The $CLint_{vitro}$ in liver cytosol ($CLint_{vitro, cys}$) was calculated using the equations below and was based on the time-course of the residual ratio of the unchanged drugs, as determined using least squares linear regression.

$CLint_{vitro, cys}$ (mL /min/mg protein) = ke / cytosolic protein concentration (2-13)

For the inhibition study, menadione (Johns, 1967), isovanillin (Beedham, 1987), and allopurinol (Massey et al., 1970), as inhibitors of AO (menadione and isovanillin) and XO respectively, were added to liver cytosol incubation mixtures at respective concentrations of 100 μmol/L.

2.3 Results

2.3.1 Pharmacokinetics of FK3453 in rats, dogs, and humans

Intravenous and oral administration of FK3453 to rats

The plasma concentration-time curve of the unchanged drug and pharmacokinetic parameters after

intravenous and oral administration to male rats are shown in Figure 2-2A and Table 2-1. Following intravenous administration at 0.1, 0.32, and 3.2 mg/kg to male rats, plasma concentrations of FK3453 decreased with respective t1/2β values of 0.95, 0.50 and 0.37 h. CLt and Vdss values at each dosage were estimated to be 14.9, 17.6, and 10.8 mL/min/kg and 0.69, 0.91, and 0.48 L/kg, respectively (Table 2-1). The pharmacokinetics of FK3453 after intravenous administration appeared to be linear within the dose range of 0.1-3.2 mg/kg in male rats. Following oral administration at 0.1, 0.32, and 3.2 mg/kg to male rats, plasma concentrations of FK3453 reached Cmax between 0.5 and 1.5 h after administration, with mean Cmax values of 41.0, 36.8, and 544.0 ng/mL, respectively. BA of FK3453 ranged from 30.5% to 41.9% in male rats (Table 2-1).

The plasma concentration-time curve of the unchanged drug and pharmacokinetic parameters after intravenous and oral administration to female rats are shown in Figure 2-2B and Table 2-1. Following intravenous administration to female rats, large individual variations were observed. The plasma concentrations of FK3453 decreased with respective t1/2β values of 1.11 and 0.36 h at 0.1 mg/kg and 1.05 and 4.49 h at 1 mg/kg, respectively. CLt and Vdss values were estimated to be 11.0, 17.2 mL/min/kg and 0.97, 0.95 L/kg at 0.1 mg/kg, and 13.7, 1.9 mL/min/kg and 0.87, 0.67 L/kg at 1 mg/kg, respectively (Table 2-1). Large individual variations were also observed following oral administration at 0.32 and 1 mg/kg to female rats. Although the mean values of Cmax and AUCinf after administration at these dosages were 73.1 and 373.3 ng/mL and 227.7 and 3372.4 ng·h/mL, respectively, individual values showed more than 5-fold variation. The BA of FK3453 ranged from 57.3% to 67.6% in female rats (Table 2-1).

A

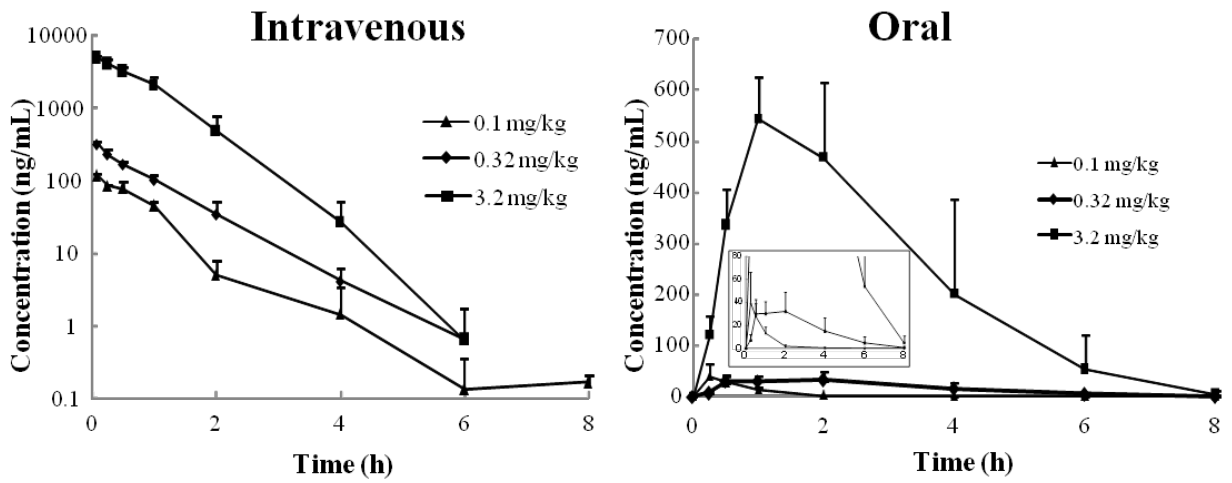

B

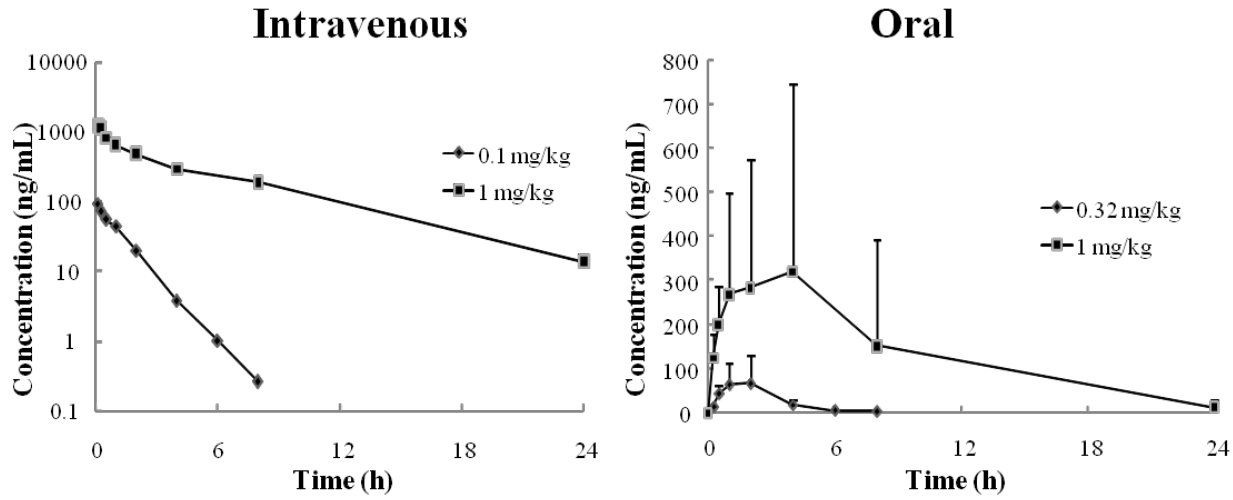

Figure 2-2. Plasma concentration-time curve of FK3453 after intravenous and oral administration to male (A) and female rats (B).

Insert is magnification for lower dose.

TABLE 2-1. Pharmacokinetic parameters of FK3453 after intravenous and oral administration to rats

	Intravenous					Oral				
	Dose *(mg/kg)*	$t_{1/2}\beta$ *(h)*	Vdss *(L/kg)*	AUCinf *(ng·h/mL)*	CLt *(mL/min/kg)*	Dose *(mg/kg)*	Cmax *(ng/mL)*	Tmax *(h)*	AUCinf *(ng·h/mL)*	BA *(%)*
Male	0.1	0.95±0.55	0.69±0.16	111.9±3.8	14.9±0.5	0.1	41.0±25.0	0.5±0.4	34.2±9.3	30.5
	0.32	0.50±0.05	0.91±0.15	304.1±23.1	17.6±1.3	0.32	36.8±11.3	1.5±0.9	127.4±71.5	41.9
	3.2	0.37±0.04	0.48±0.06	5170.3±1502.9	10.8±2.7	3.2	544.0±82.8	1.0±0.0	1789.4±600.3	34.6
Female	0.1	0.73 <1.11, 0.36>	0.96 <0.97, 0.95>	124.2 <151.3, 97.2>	14.1 <11.0, 17.2>	0.32	73.1±58.6 <47.1, 140.2, 31.9>	1.2±0.8 <0.5, 2, 1>	227.7±187.3 <139.5, 442.9, 100.8>	57.3 [a]
	1	2.77 <1.05, 4.49>	0.77 <0.87, 0.67>	4987.2 <1217.5, 8756.9>	7.8 <13.7, 1.9>	1	373.3±382.3 <175.0, 814.0, 131.0>	1.7±2.0 <0.5, 4, 0.5>	3372.4±4635.5 <752.2, 8724.6, 640.4>	67.6

[a] Bioavailability calculated from 124.2 and 227.7 ng·h/mL (corrected for dose); for all other instances, bioavailability was calculated using AUCinf among same dosage.

Data represent mean ± SD for n =3 unless stated. Mean values for n=2 and individual values are listed for intravenous administration to female rats, and mean ± SD for n=3 and individual values are listed for oral administration, also to female rats.

Intravenous and oral administration of FK3453 to dogs

The plasma concentration-time curve of the unchanged drug and pharmacokinetic parameters after intravenous and oral administration to dogs are shown in Figure 2-3 and Table 2-2. Following intravenous administration at 0.1 mg/kg to dogs, the mean values of CLt, Vdss, t1/2β, and AUCinf were 5.0 mL/min/kg, 0.87 L/kg, 2.7 h, and 339.7 ng·h/mL, respectively (Table 2-2). Following oral administration at 0.03, 0.1, and 0.3 mg/kg to dogs, plasma concentrations of FK3453 reached Cmax between 0.5 and 1 h after administration, with mean Cmax values of 19.2, 70.4, and 252.3 ng/mL, respectively. Mean BA of FK3453 ranged from 71.3% to 93.4% in dogs (Table 2-2). The pharmacokinetics of FK3453 after oral administration appeared to be linear within the does range of 0.03-0.3 mg/kg in dogs.

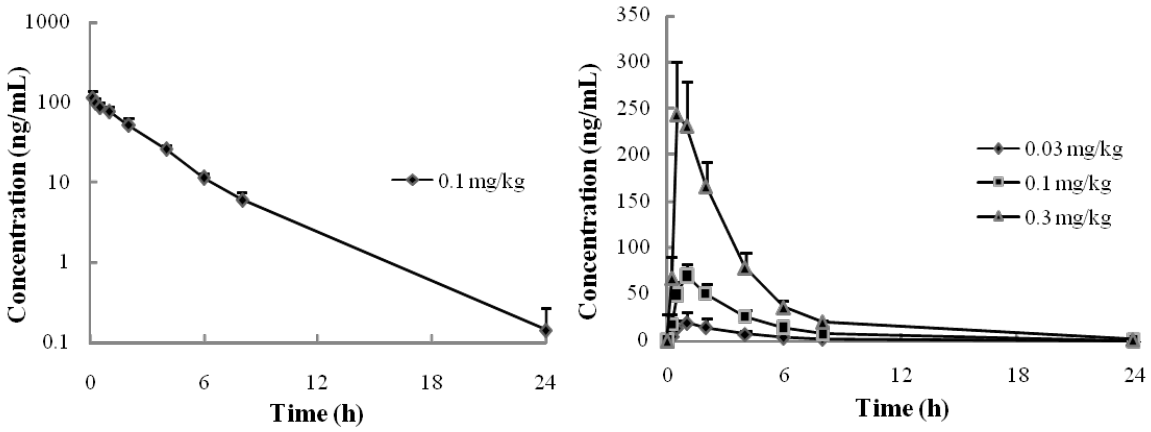

Figure 2-3. Plasma concentration-time curve of FK3453 after intravenous and oral administration to dogs.

TABLE 2-2. Pharmacokinetic parameters of FK3453 after intravenous and oral administration to dogs

	Dose *(mg/kg)*	$t_{1/2}\beta$ *(h)*	Vdss *(L/kg)*	AUCinf *(ng·h/mL)*	CLt *(mL/min/kg)*	Cmax *(ng/mL)*	Tmax *(h)*	BA *(%)*
Intravenous	0.1	2.7±0.8	0.87±0.03	339.7±52.0	5.0±0.8	-	-	-
Oral	0.03	-	-	72.9±17.7	-	19.2±2.8	1.0±0.0	71.3±9.8
	0.1	-	-	299.8±81.1	-	70.4±11.2	1.0±0.0	87.1±12.3
	0.3	-	-	953.6±161.0	-	252.3±59.6	0.7±0.3	93.4±2.3

Data represent mean ± SD for n =3

Oral administration of FK3453 to humans

The plasma concentrations and pharmacokinetic parameters of the unchanged drug after oral administration at 0.5, 1, and 10 mg to humans are shown in Table 2-3. The plasma concentration-time curves of FK3453 and M4 for 10 mg administration are shown in Figure 2-4, and the plasma concentrations and pharmacokinetic parameters of M4 are shown in Table 2-4. Following oral administration to humans, the unchanged drug was detected in only slight amounts in human plasma at all time-points for all doses (Table 2-3). In contrast, high concentrations of M4 were observed in human plasma at 10 mg (Table 2-4). The Cmax and AUCinf values of M4 were approximately 200 times greater than those of FK3453.

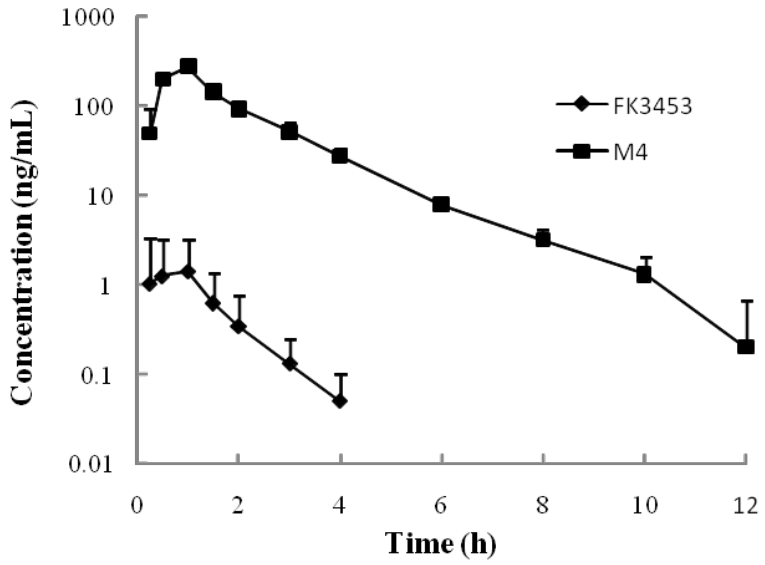

Figure 2-4. Plasma concentration-time curve of FK3453 and M4 after oral administration at 10 mg to humans.

TABLE 2-3. Plasma concentration of FK3453 after oral administration to humans

Dose (mg)	Subject No.	Plasma concentration (ng/mL)								Cmax (ng/mL)	AUC0-6 (ng·h/mL)
		Pre	*0.25 h*	*0.5 h*	*1 h*	*1.5 h*	*2 h*	*3 h*	*4 h*		
0.5	2	n.d.	0.055	0.257	0.222	0.112	0.056	n.d.	n.d.	0.257	0.319
	4	n.d.	n.d.	0.065	0.069	0.037	0.026	n.d.	n.d.	0.069	0.097
	5	n.d.	n.d.	n.d.	n.d.	n.d.	n.d.	n.d.	n.d.	0.000	0.000
	6	n.d.	n.d.	0.055	0.033	n.d.	n.d.	n.d.	n.d.	0.055	0.037
	7	n.d.	0.025	0.154	0.060	n.d.	n.d.	n.d.	n.d.	0.154	0.094
	8	n.d.	0.133	0.103	0.039	n.d.	n.d.	n.d.	n.d.	0.133	0.091
	Mean	0.000	0.036	0.106	0.071	0.025	0.014	0.000	0.000	0.111	0.106
	S.D.	0.000	0.052	0.090	0.078	0.045	0.023	0.000	0.000	0.090	0.111
1	10	n.d.	n.d.	0.060	0.085	0.093	0.074	0.321	0.075	0.321	0.601
	11	n.d.	n.d.	0.152	0.093	0.029	n.d.	n.d.	n.d.	0.152	0.118
	13	n.d.	0.082	0.182	0.062	0.028	n.d.	n.d.	n.d.	0.182	0.134
	14	n.d.	n.d.	0.173	0.205	0.116	0.091	0.029	n.d.	0.205	0.323
	15	n.d.	0.057	0.353	0.179	0.097	0.046	n.d.	n.d.	0.353	0.319
	16	n.d.	0.070	0.148	0.081	0.029	n.d.	n.d.	n.d.	0.148	0.128
	Mean	0.000	0.035	0.178	0.118	0.073	0.035	0.058	0.013	0.227	0.270
	S.D.	0.000	0.039	0.096	0.059	0.041	0.041	0.129	0.031	0.088	0.188
10	17	n.d.	0.051	0.452	1.167	0.460	0.231	0.106	0.051	1.167	1.352
	18	n.d.	0.073	0.215	0.238	0.121	0.073	0.032	n.d.	0.238	0.365
	19	n.d.	0.109	0.374	0.321	0.169	0.066	0.028	n.d.	0.374	0.490
	22	n.d.	0.067	0.503	0.705	0.486	0.331	0.172	0.064	0.705	1.317
	23	n.d.	0.282	0.645	0.889	0.344	0.177	0.076	0.036	0.889	1.192
	24	n.d.	5.643	5.325	5.081	2.139	1.130	0.353	0.139	5.643	8.427
	Mean	0.000	1.038	1.252	1.400	0.620	0.335	0.128	0.048	1.503	2.190
	S.D.	0.000	2.258	2.000	1.836	0.759	0.402	0.122	0.052	2.056	3.085

n.d.:<0.025 ng/mL, Plasma concentrations of FK3453 were below the detection limit at 6 or more hours after administration at all doses.

TABLE 2-4. Plasma concentrations of M4 after oral administration at 10 mg of FK3453 to humans

Dose	Subject	Plasma Concentration (ng/mL)											Cmax	AUC0-24
(mg)	**No.**	*Pre*	*0.25 h*	*0.5 h*	*1 h*	*1.5 h*	*2 h*	*3 h*	*4 h*	*6 h*	*8 h*	*10 h*	*12 h*	*(ng/mL)*	*(ng·h/mL)*
10	17	-	10.5	157.8	367.6	141.8	80.5	51.6	29.0	7.9	2.8	1.2	n.d.	367.6	495.8
	18	-	38.4	196.0	276.5	160.2	90.2	50.1	28.6	8.7	3.5	1.5	n.d.	276.5	489.5
	19	-	52.2	255.2	226.9	119.1	94.4	40.7	23.6	6.8	2.5	1.1	n.d.	255.2	449.5
	22	-	9.7	146.2	215.6	147.5	126.3	73.6	29.4	10.2	3.6	1.6	n.d.	215.6	482.0
	23	-	59.3	202.8	304.8	142.1	95.5	53.9	34.3	8.6	4.5	2.4	1.2	304.8	530.7
	24	-	124.1	223.4	235.9	136.2	65.1	31.8	15.8	4.7	1.8	n.d.	n.d.	235.9	418.2
	Mean	-	49.0	196.9	271.2	141.2	92.0	50.3	26.8	7.8	3.1	1.3	0.2	275.9	477.6
	S.D.	-	42.2	40.6	57.9	13.5	20.3	14.1	6.4	1.9	0.9	0.8	0.5	54.6	39.1

n.d.:<1 ng/mL

-:Not determined

Plasma concentrations of M4 were below the detection limit at 24 or more hours after administration at all doses.

2.3.2 *In vitro* parameters

Data regarding protein binding, RB, and $CLint_{vitro,\ liver}$ of FK3453 in male rats, dogs, and humans are shown in Tables 2-5 and 2-6. The percent-bound values for FK3453 were similar in all species examined over a concentration range of 2 to 200 ng/mL, ranging from 74.78% to 75.83% in male rats, 67.87% to 68.75% in dogs, and 75.47% to 77.56% in humans (Table 2-5). The blood to plasma concentration ratio of FK3453 was also similar in all species examined over the concentration range of 2 to 200 ng/mL, ranging from 0.86 to 0.89 in male rats, 0.89 to 0.99 in dogs, and 0.78 to 0.82 in humans (Table 2-5). $CLint_{vitro,\ liver}$ values of FK3453 in male rat, dog, and human were 42.3, 14.5, and 1.1 mL/min/kg, respectively (Table 2-6).

2.3.3 Prediction of human hepatic availability from *in vitro-in vivo* scaling

The $CLint_{vivo}$ values in male rats and dogs were calculated to be 51.3-94.5 and 17.8, respectively, and the predicted human Fh was estimated to be >0.97 (Table 2-6).

TABLE 2-5. Summary of protein binding and blood to plasma concentration ratio of FK3453 in male rats, dogs and monkeys

Species	Protein binding		Rb	
	(ng/mL)	*(%)*	*(ng/mL)*	*(%)*
Male rats	2	74.78	2	0.87
	20	75.83	20	0.86
	200	75.37	200	0.89
Mean		75.33		0.87
Dogs	2	67.87	2	0.99
	20	68.56	20	0.93
	200	68.75	200	0.89
Mean		68.39		0.94
Humans	2	75.47	2	0.82
	20	77.56	20	0.82
	200	77.23	200	0.78
Mean		76.75		0.81

Rb, blood-to-plasma concentration ratio

Data in each concentration represent mean for n =3.

TABLE 2- 6. Estimation of Fh in humans from *in vitro* and *in vivo* intrinsic clearance in male rats and dogs

	Animals			Scaling Factor	Humans		
	Dose *(iv, mg/kg)*	CLint $_{vitro}$ *(mL/min/kg)*	CLint $_{vivo}$ *(mL/min/kg)*		CLint $_{vitro}$ *(mL/min/kg)*	CLint $_{vivo}$ [a] *(mL/min/kg)*	Fh [a]
Male rats	0.1	42.3	76.0	1.80	1.1	2.0	0.97
	0.32		94.5	2.23		2.5	0.97
	3.2		51.3	1.21		1.3	0.98
Dogs	0.1	14.5	17.8	1.23		1.4	0.98

[a] Predicted values

2.3.4 Identification of mechanism responsible for low exposure of FK3453 in humans

In vitro *metabolite profile study*

After incubation of [^{3}H]-FK3453 with human sub-cellular liver fractions, at least six peaks derived from FK3453 metabolites were observed on the radio-chromatograms. Although the major metabolite of FK3453 was M4, three others in the incubation mixture were also identified as the dealkylated metabolite on the nitrogen in the pyridazine (M1), hydroxylated metabolite on the isopropyl group (M2), and p-hydroxylated metabolite on the benzene ring (M3) (Fig. 2-5). Although M4, the main metabolite in human plasma, was not detected in the incubation mixture with microsomes (Fig. 2-6), it was detected in the mixture with S9 (Fig. 2-7A). In the inhibition study, the metabolic reaction of M4 formation was inhibited by menadione (Fig. 2-7C) but not 1-aminobenzotriazole or allopurinol (Fig. 2-7B, D).

In vitro *metabolic inhibition study with liver cytosol*

CLint $_{vitro,\ cys}$ values of FK3453 in male rat, female rat, and human were 1.1, 12.5, and 6.5 mL/min/mg protein, respectively. These metabolic reactions were inhibited by menadione and isovanillin but not allopurinol (Table 2-7, Fig. 2-8). Whereas, no depletion of FK3453 was observed in dog liver cytosol (Table 2-7).

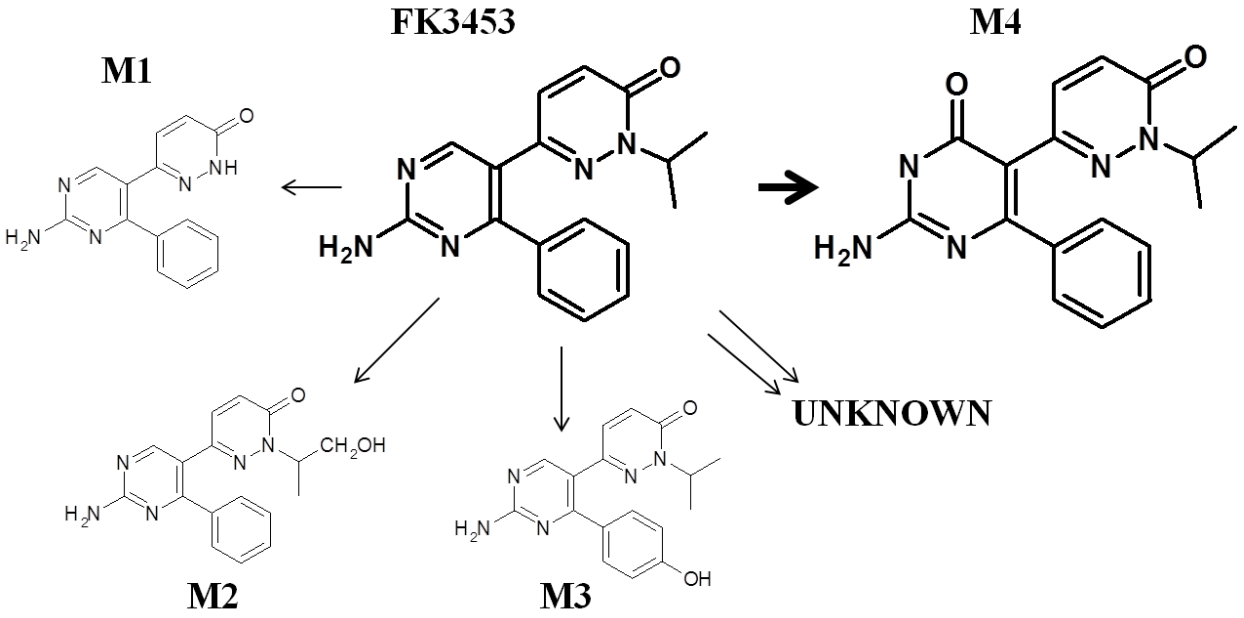

Figure 2-5. Possible metabolic pathway of FK3453 in incubation mixture with human liver sub-cellular fractions.

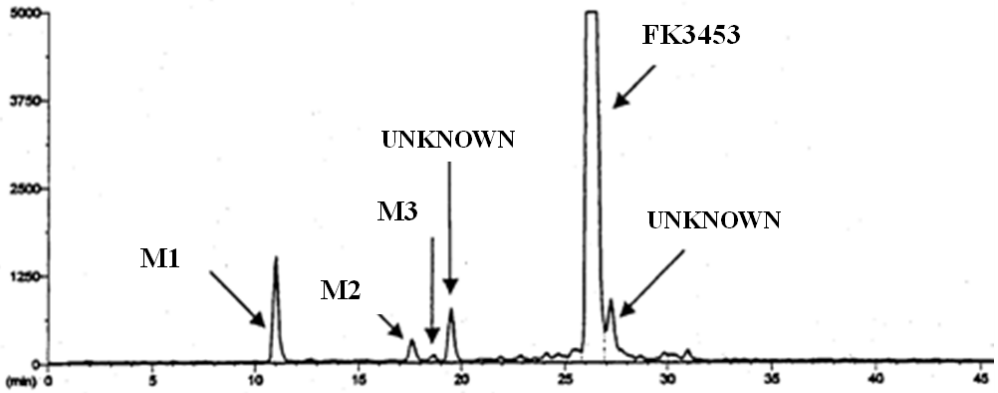

Figure 2-6. Representative HPLC radio-chromatogram of reaction mixture after incubation of [^{3}H]-FK3453 with human liver microsomes.

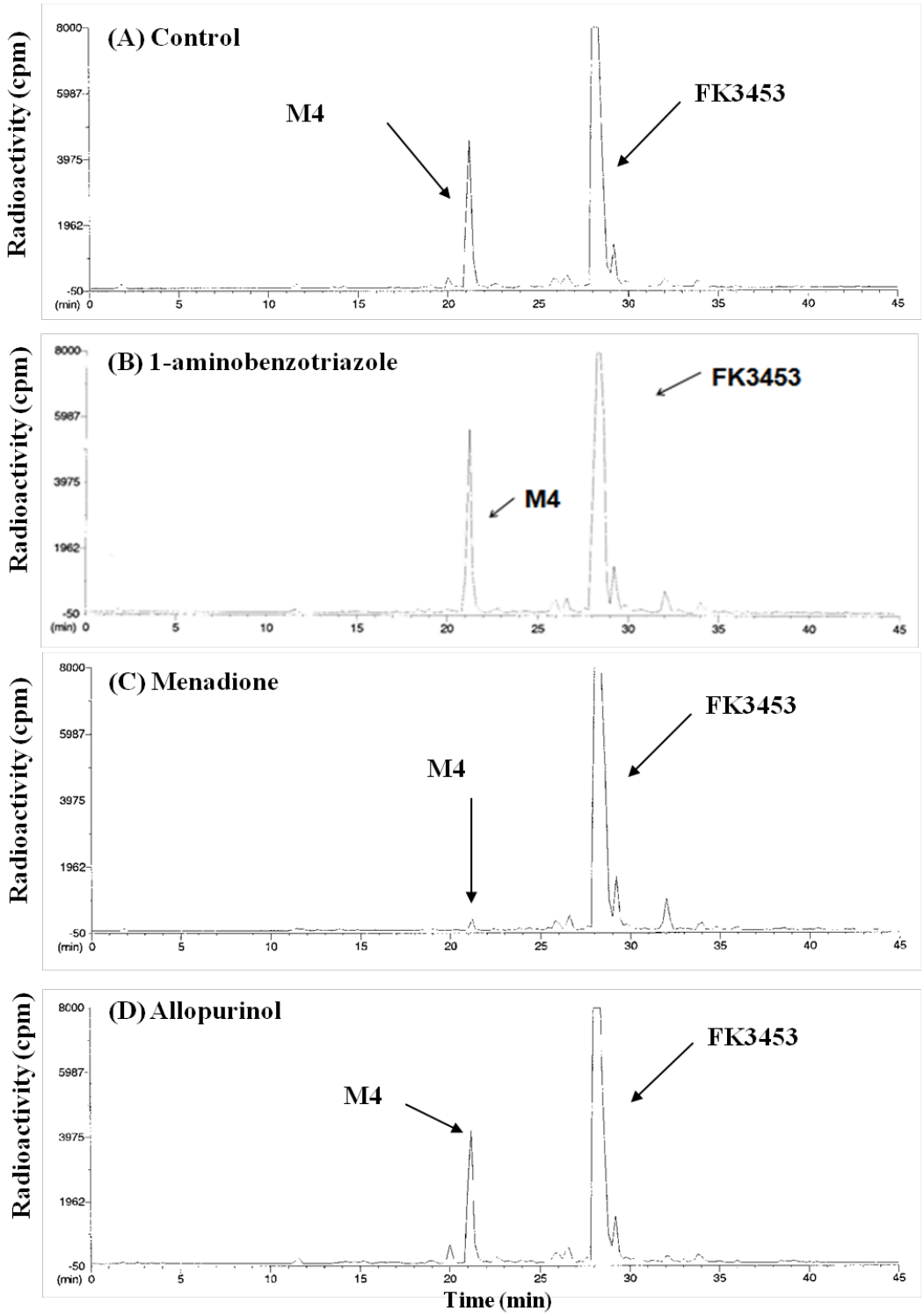

Figure 2-7. Representative HPLC radio-chromatogram of reaction mixture after incubation of [^{3}H]-FK3453 with human liver S9 and inhibitors.

(A) control, without inhibitor; (B) 1-aminobenzotiazole, CYP inhibitor; (C) menadione, aldehyde oxidase inhibitor; (D) allopurinol, xanthine oxidase inhibitor.

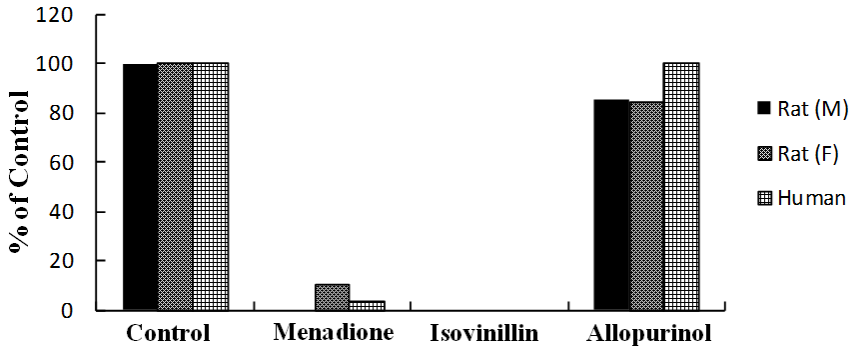

Figure 2-8. Percentage of remaining cytosolic enzyme activity to the control (without inhibitors) in presence of aldehyde oxidase inhibitors (menadione and isovanillin) or xanthine oxidase inhibitor (allopurinol) in male rats, female rats, and humans.

TABLE 2-7. *In vitro* metabolic inhibition study using male rats, female rats, dogs and humans liver cytosol.

Species	CLint $_{vitro,\ cys}$ (mL/min/mg protein)			
	Control	Menadione	Isovanillin	Allopurinol
Male rats	1.1	ND	ND	0.9
Female rats	12.5	1.3	ND	10.5
Dogs	ND	ND	ND	ND
Humans	6.5	0.2	ND	6.5

CLint $_{vitro,\ cys}$, *in vitro* intrinsic clearance calculated from cytosol study; ND, No depletion

2.4 Discussion

I described the *in vitro* and *in vivo* pharmacokinetic profiles of FK3453 in rats, dogs, and humans, and investigated the mechanism responsible for low exposure of the unchanged drug in humans. The predicted human Fh estimated from pharmacokinetic parameters in male rats and dogs exceeded 0.97 (Table 2-6), suggesting a favorable pharmacokinetic profile of FK3453 in humans. However, poor systemic exposure of FK3453 was observed after oral administration to humans in a phase 1 study (Table 2-3). As a consequence, I failed to predict the pharmacokinetics of FK3453 in humans from preclinical data.

To clarify the principal factor responsible for low systemic exposure of FK3453 in humans, I assessed the pharmacokinetic properties of FK3453 from various aspects. In terms of absorption, I predicted favorable absorption from the gastrointestinal tract based on observations of good solubility, high membrane permeability (data not shown), and high BA in rats and dogs. To investigate the metabolite profile in human plasma, I measured circulating metabolites of FK3453 in a phase 1 study, identifying M4, an oxidative metabolite of the aminopyrimidine moiety, as a major metabolite with Cmax and $AUC_{0\text{-}t}$ values approximately 200-fold greater than those of FK3453 at 10 mg oral administration. The high plasma levels of M4 strongly suggested that extensive metabolism for M4 formation was a major factor in the low systemic exposure of FK3453. M4 is an oxidative metabolite of FK3453 with structural characteristics suggesting the involvement of AO and XO, molybdenum cofactor-containing soluble enzymes which catalyze oxidation of compounds such as aldehyde and N-heterocyclic aromatic compounds (Kitamura et al.,

2006).

I then investigated the possible involvement of AO or XO in M4 formation. As AO and XO are cytosolic enzymes, I used liver S9 and liver microsomes to conduct our *in vitro* metabolic assay to investigate the sub-cellular location of enzymes involved in M4 formation. After separately incubating [^{3}H]-FK3453 with human liver S9 and microsomes, M4 formation was observed in the reaction mixture incubated with S9 but not in that with microsomes (Fig. 2-6, 2-7A), which suggested the involvement of cytosolic enzymes such as AO or XO in M4 formation. This then prompted our examination of the inhibitory effect on M4 formation in an effort to identify the enzyme responsible for M4 formation between AO, XO, or any other CYPs. For this study, I selected 1-aminobenzotriazole, menadione and allopurinol as potent inhibitors of CYPs, AO, and XO, respectively, and found that M4 formation was inhibited by menadione but not by allopurinol or 1-aminobenzotriazole (Fig. 2-7). A similar results were also observed in the metabolic inhibition study using liver cytosol (Table 2-7, Fig. 2-8). These results indicated that the enzyme responsible for converting FK3453 to M4 was AO, and the low systemic exposure of FK3453 in humans was due to unpredictably high AO metabolism.

Although AO is known to catalyze oxidation of several clinical drugs, including zaleplon, methotrexate, and ziprasidone (Beedham et al., 2003; Kawashima et al., 1999; Kitamura et al., 1999), few reports have explored AO metabolism with regard to human pharmacokinetic prediction and species differences (Zientek et al., 2010; Diamond et al., 2010). Difficulties in understanding AO metabolism may be explained by several key reasons. Chiefly, large variations in AO activity

had been observed between rat strains (Sugihara et al., 1995; Sasaki et al., 2006), and a significant genetic polymorphisms had also been identified even among members of the same strains (Itoh et al., 2007a, b). These findings suggest that diligent care must be taken in selecting rat strains to be used in evaluating the pharmacokinetic profile of drug candidates metabolized by AO. Indeed, I did observe large pharmacokinetic variation in female rats in the present study (Fig. 2-2B). In contrast, deficiency of AO expression was reported in dogs (Kitamura et al., 1999; Diamond et al., 2010). I observed a good pharmacokinetic profile for FK3453 in dogs and no cytosolic enzyme reaction in dogs, findings which were highly consistent with reports of absence of AO metabolism in dogs. These results suggest that conventional preclinical animal pharmacokinetic studies such as rat- and dog-based studies are not sufficiently fulfilled to evaluate the *in vitro-in vivo* relationship for AO metabolism and to predict the human pharmacokinetic profile (Dalvie et al., 2010). Instead, given that high AO activity has been reported in monkeys (Diamond et al., 2010), monkeys may be useful as a preclinical species assessing AO metabolism. However, a large species difference in pharmacokinetic profile was also reported between humans and cynomolgus monkeys following oral administration of several drugs mainly metabolized by CYPs (See Chapter 1). For this reason, special care should be focused on the metabolic enzymes of a drug candidate if monkeys are used in pharmacokinetic studies in drug discovery research.

Another problem with regard to predict AO metabolism in human is that conventional *in vitro* studies such as general metabolic stability screening using liver microsomes may lead to underestimation of the risk of AO metabolism of drug candidates in humans, as AO is located in the

cytosol. In addition, unlike CYP metabolism, methods of predicting human pharmacokinetics for metabolism by cytosolic enzymes have not been well established. A possible way to predict the human hepatic availability of cytosolic enzymes substrates is an *in vitro-in vivo* scaling using the data obtained from incubation with cytosol or S9 fractions. Zientek et al (2010) reported *in vitro-in vivo* correlations (IVIVC) for AO substrates using human liver cytosol and S9, however, the underestimation of human hepatic availability was also observed. Furthermore, Zientek et al (2010) discussed that one reason for underestimation of human hepatic availability was attributed to enzymatic lability of AO during homogenization and storage process. Therefore, further preclinical study using monkeys or *in vitro* studies using more comprehensive evaluation tools such as human hepatocytes will be necessary to facilitate a better understanding of AO metabolism.

In summary, I demonstrated that the poor systemic exposure of FK3453 observed in humans was due to unpredictably high AO metabolism despite the favorable pharmacokinetic profiles FK3453 showed in rats and dogs.

3. A quantitative approach to hepatic clearance prediction of metabolism by aldehyde oxidase using pooled hepatocytes.

3.1 Introduction

While the prediction of *in vivo* hepatic clearance in humans from $CLint_{vitro,\ liver}$ has been closely studied for compounds cleared by CYP, microsome-based methods do not adequately describe total metabolic activity, and non-CYP metabolism is now of increasing concern in human pharmacokinetic prediction. Indeed, the risk of underestimating AO metabolism in humans was suggested in Chapter 2. This situation indicates the need for novel approaches to complement microsome-based prediction methods for human AO metabolic pathways.

With their broad spectrum of enzyme activity, human hepatocytes have garnered recent attention as a novel tool for evaluating metabolism to complement liver sub-cellular fractions such as microsomes, cytosol, and S9 fractions. Human hepatocytes have been found to be a physiologically relevant tool for evaluating liver-related pharmacokinetics, including metabolism, drug-drug interaction, and drug transport (Li, 2007, 2010; Soars et al., 2007, 2009), and both fresh and cryopreserved human hepatocytes are used in various circumstances. Cryopreserved hepatocytes might have similar usability as human liver sub-cellular fractions in aspects such as long-term storage, ease of experimental scheduling, choice of pre-characterized lots for experimentation, and repeat experimentations with hepatocytes from the same donors (Li et al., 2010), and these aspects would prove extremely useful in drug discovery screening. Thus,

cryopreserved hepatocytes might prove a useful tool in the comprehensive evaluation of metabolism at drug discovery, including AO metabolism. In addition, since the use of individual cryopreserved hepatocytes lots for large-scale compound metabolic screening studies might be hampered by lot-to-lot individual variation and a limited number of vials, pooled hepatocytes aimed at overcoming these disadvantages have been developed. Among advantages, pooled hepatocytes provide a far larger number of vials from the same lot than samples from individuals. This potentially allows large-scale metabolic studies, such as metabolic stability screening, drug-drug interaction, and hepatic clearance prediction, provided the same lot of hepatocytes can be used for a certain length of time. However, using cryopreserved hepatocytes to improve understanding of AO metabolism in humans will require that the AO enzymatic activity of fresh hepatocytes is maintained in cryopreserved ones, or pooled hepatocytes maintain the average AO activity of each of the individual lots which comprise the pooled hepatocytes. However, information concerning the effect of the production process of cryopreserved hepatocytes or pooled hepatocytes on AO activity is unknown.

In this study, to confirm the usefulness of human hepatocytes in evaluating AO metabolism, I firstly compared the CLint values of 4 compounds primarily metabolized by AO in freshly isolated and cryopreserved hepatocytes from the same donor (n=4). Subsequently, I compared CLint values of AO substrates in individual lots and in pooled hepatocytes consisting of lots from the same individual donors. I then examined a quantitative prediction for human hepatic clearance in AO substrates using CLint in pooled hepatocytes and CLint $_{vivo}$ calculated from clinical data in the

literature.

3.2 Materials and Methods

3.2.1 Chemicals and reagents

FK3453 was synthesized at Astellas Pharma Inc (Osaka). XK-469 (XK), o6-benzylguanine (O6BG), phthalazine (PHT) was purchased from Sigma-Aldrich Corporation. Zaleplon (ZAL), and 6-deoxypenciclovir (6DP) were purchased from Toronto Research Chemicals Inc. (Ontario, Canada).Zoniporide (ZNP) was purchased from Tocris Bioscience, LLC (Ellisville, MO). The structure of each compound is shown in Figure 3-1. William Medium E and Cryopreserved Hepatocytes Recovery Medium (CHRM®) were purchased from CellzDirect/Invitrogen Corporation (Durham, NC). All other reagents and solvents were commercial products of analytical grade.

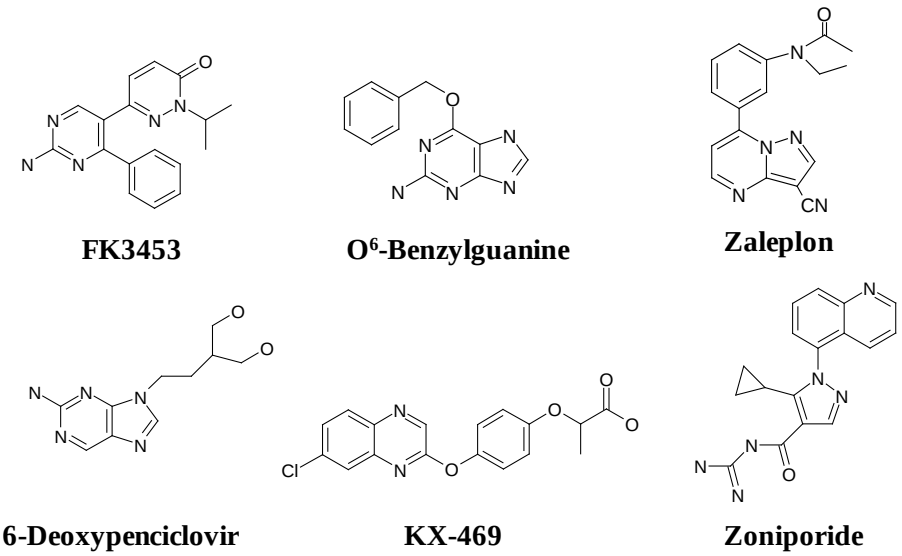

Figure 3-1. Structure of each AO-cleared compound.

3.2.2 Human hepatocytes

Cells

Freshly isolated and cryopreserved hepatocytes were purchased from CellzDirect/Invitrogen Corporation (lot names Hu1186 and Hu1197) and Celsis In Vitro Technologies (lot names SLH and EXG; Baltimore, MD, USA). Cryopreserved hepatocytes (lot names GGJ, IQJ, TSF, and WMN), and custom pooled hepatocytes consisting of the four lots described above (lot name: VKA) were also purchased from Celsis In Vitro Technologies.

Fresh human hepatocytes study

Hepatocytes were re-suspended in pre-warmed William Medium E containing HEPES (final concentration: 15 mM) and L-glutamine (final concentration: 2 mM) purged with 95% O_2 and 5% CO_2 (pH: 7.2-7.4). Cell viability was assessed via trypan blue exclusion just prior to and after incubation. Hepatocytes showing >80% viability before and >60% viability after incubation were used.

Cryopreserved human hepatocytes study

The hepatocytes were stored in liquid nitrogen until use, at which point they were removed from the liquid nitrogen and immediately immersed in a water bath pre-warmed to 37 °C. The vials were shaken gently until all ice crystals had been dissolved and then emptied into pre-warmed CHRM®. After centrifugation at 100 × *g* for 10 min at room temperature, the hepatocytes were re-suspended

in pre-warmed William Medium E containing HEPES (final concentration: 15 mM) and L-glutamine (final concentration: 2 mM) purged with 95% O_2 and 5% CO_2 (pH: 7.2-7.4). Cell viability was assessed as described above.

3.2.3 In vitro metabolism in hepatocyte suspensions

Metabolic study conditions

Each compound and cells in suspension buffer were pre-incubated separately at 37 °C for 10 min in a 5% CO_2 incubator (MCO-18AIC; SANYO Electric Co. Ltd., Osaka), after which reactions were initiated by adding cell suspensions solution (final concentration of hepatocytes: 0.1 million cells/mL for PHT; 0.5 million cells/mL for FK3453 and O6BG; 1 million cells/mL for 6DP, ZAL, and ZNP; and 2.5 million cells/mL for XK.) to compound solution (final concentration of each compound: 0.2 μM, total ratio of organic solvent in incubation mixture: <0.5%).

Reactions were terminated by adding reaction mixture to ice-cold acetonitrile with 0.1% formic acid (v/v), including the internal standard, at 0, 30, 60, 90, and 120 min. After terminating the metabolic reaction, the reaction mixtures of all compounds were centrifuged at 1,500 × *g* for 5 min. The supernatant was then decanted and 50 μL of 0.1% formic acid was added, after which 2- to 5-μL aliquots of the resulting solutions were subjected to LC-MS/MS. Each assay was performed in triplicate.

LC-MS/MS conditions

The amount of unchanged compounds was determined using LC-MS/MS analysis. The mass numbers of the molecular and product ions for each compound were identified as follows (polarity, molecular>product): FK3453 *m/z* = 308 > 266 [M+H]+; O6BG *m/z* = 242 > 91 [M+H]+ ; PHT *m/z* = 131 > 104 [M+H]+; ZAL *m/z* = 306 > 236 [M+H]+; 6DP *m/z* = 238 > 136 [M+H]+; XK *m/z* = 345 > 273 [M+H]+; ZNP *m/z* = 321 > 262 [M+H]+.

The Prominence 2000 series (Shimadzu) was used as the LC-system. MS/MS analyses were conducted on an API-5000 MS/MS system (AB SCIEX). A n Atlantis® C18 (5 μm, 2.0 x 50 mm; Waters Corporation, Milford, MA, USA) for 6DP. An XBridge™ C18 (5 μm, 2.0 x 50 mm; Waters Corporation) HPLC column was used for all other compounds. Mobile phase was 0.1% formic acid and acetonitrile, and gradient elution was carried out for all LC-MS/MS analyses.

Calculation of in vitro *intrinsic clearance*

The $CLint_{vitro}$ in hepatocytes ($CLint_{vitro, hep}$) was calculated using Equation 3-1 and 3-2 based on the time course of the residual ratio of the unchanged compounds (%), as determined using least squares linear regression (Naritomi et al. 2001). The depletion profile of unchanged compounds is described as follow if substrate disappearance rate can be assumed to follow first order kinetics

$$R(t) = 100 \cdot \exp(-ke \cdot t) \quad (3\text{-}1)$$

$CLint_{vitro, hep}$ (μL/min/million cells) = ke (min^{-1}) / cell concentration (million cells/mL)× 1000 (3-2),

where R(t) is the residual ratio of the unchanged compounds (%) at each incubation time (time 0 was regarded as 100%), ke is the disappearance rate constant of unchanged compounds.

For IVIVE analysis, the units of $CLint_{vitro, hep}$ values were then converted to per kilogram of body weight using Equation 3-3.

$CLint_{vitro, hep}$ (mL/min/kg)

= $CLint_{vitro, hep}$ (mL/min/million cells) x *SF1* (million cells/g liver) x *SF2* (g liver/kg body weight) (3-3)

where *SF1* is the number of cells per gram of liver and *SF2* is the liver weight per kilogram of body weight. (120 and 25.7 were used, respectively; Naritomi et al. 2003).

$CLint_{vitro, hep}$' is *in vitro* intrinsic clearance corrected by unbound fraction in hepatocyte incubation (fu_{hep}; See Unbound fraction in hepatocyte incubation under Materials and Methods, Equation 3-4).

$CLint_{vitro, hep}$' (mL/min/kg) = $CLint_{vitro, hep}$ (mL/min/kg) / fu_{hep} (3-4)

3.2.4 *In vitro* parameters

Blood-to-plasma concentration ratio

Three hundred microliters of human blood was spiked with 3 μL of 100 μM standard solution (1 μM final) and pre-incubated in a shaking water bath at 37 °C for 30 min. A 25-μL aliquot was then

taken as a blood sample. The remaining samples were centrifuged at 4 °C and 1,800g for 10 min, after which a 25-μL aliquot of plasma sample was taken. Samples (25 μL of sample plasma and 25 μL of blank blood or 25-μL of sample blood and 25-μL of blank plasma) were quenched with 200 μL of ice-cold acetonitrile containing internal standard and centrifuged at 10,000g for 5 min. The Rb was then calculated from the peak area of compounds to that of the internal standard in blood per that in plasma. Each assay was performed in triplicate. A value of 0.55 (1 - hematocrit) was used if the calculated Rb value was less than 0.55.

Plasma protein binding

Protein binding was determined using a rapid equilibrium dialysis device (Pierce Biotechnology, Thermo Fisher Scientific, Waltham, MA, USA) method (Waters et al., 2008) and an ultracentrifugation method with the following equations:

$$\text{Protein binding (\%)} = (1\text{-fp}) \times 100 \qquad (3\text{-}5)$$

$$\text{fp} = \text{concentration in PBS or supernatant/concentration in serum} \qquad (3\text{-}5)'$$

where fp is the unbound drug fraction in plasma. The unbound drug fraction in blood (fb) was calculated by dividing fp by Rb.

The rapid equilibrium dialysis method was used to determine the protein binding of XK-469, and the ultracentrifugation method was used for all other AO substrates.

Rapid equilibrium dialysis method

Aliquots (1 mL) of human plasma were spiked with 10 μL of 100 μg/mL standard solution (1 μg/mL final). 300-μL aliquots of the spiked plasma were then added to the donor wells (n=3), and 500-μL aliquots of PBS were added to the acceptor wells. The plate was then sealed and incubated on an orbital shaker (120 rpm) at 37 °C overnight (13-16 h).

Incubation samples (10 μL of sample plasma and 100 μL of blank PBS, or 100 μL of sample PBS and 10 μL of blank plasma) were quenched with 200 μL of ice-cold acetonitrile containing internal standard and centrifuged at 10,000g for 5 min. The supernatant was removed under a stream of nitrogen gas, the residue was then dissolved in 150 μL of mobile phase, and a 2-5-μL aliquot was injected into LC-MS/MS.

Ultracentrifugation method

Aliquots (1 mL) of human plasma were spiked with 10 μL of 100-μg/mL standard solution (1 μg/mL final). The calibration samples were prepared by adding 17 μL of 50% acetonitrile to 1,700 μL of human plasma. These samples were then centrifuged at 436,000g for 140 min at 37 °C using a Beckman Optimal TL ultracentrifuge (Beckman Coulter, Fullerton, CA, USA). After ultracentrifugation, the fp was calculated by dividing the concentration of drugs in the supernatant by that in the plasma. The assay was performed in triplicate.

Unbound fraction in hepatocyte incubation

The unbound fraction in hepatocyte incubation (fu_{hep}) was determined using the rapid equilibrium

dialysis method (Pierce Biotechnology, Thermo Fisher Scientific). Aliquots (1 mL) of hepatocyte suspensions were spiked with 10 μL of 20-μM standard solution (0.2 μM final), then 300-μL aliquots of the spiked hepatocyte suspensions were added to the donor wells (n=3), after which 500-μL aliquots of William Medium E containing HEPES (final concentration: 15 mM) and L-glutamine (final concentration: 2 mM) were added to the acceptor wells. The cell concentration of each compound was consistent with that in the metabolic study (described below). The plate was sealed and incubated on an orbital shaker (120 rpm) at 37 °C for 6 h.

After incubation, 200 μL of ice-cold acetonitrile containing internal standard was added to the incubation samples (30 μL of sample suspension and 30 μL of blank medium, or 30 μL of sample medium and 30 μL of blank suspension) and centrifuged at 10,000g for 5 min. The supernatant was removed under a stream of nitrogen gas, the residue was dissolved in 150 μL of mobile phase, and 2-5-μL aliquots were injected into LC-MS/MS. The fu_{hep} was then calculated from the peak area of compounds to that of the internal standard in sample medium per that in sample suspensions. A value of 1 was used if calculated fu_{hep} was greater than 1.

3.2.5 Data analysis

Statistical Analysis

Homogeneity of variances was analyzed using the F test at $P<0.05$ (two-tailed test). If a set of variances was found to be homogenous, Student's t test was used at $P<0.05$ (two-tailed test). Significance of differences in average value of $CLint_{vitro,\ hep}$ between freshly isolated and

cryopreserved hepatocytes was determined using an unpaired Student's t test; significance of differences in matching lots was determined using a paired Student's t test.

Calculation of CLint $_{\text{vivo}}$ *for IVIVC*

The CLint $_{vivo}$ was calculated using the following equations, based on the dispersion model (Iwatsubo et al., 1996):

$$CLh = CLt - CLr,\ CLt \times (1\text{-}fe),\ \text{or Dose iv/AUC iv} \qquad (3\text{-}6)$$

$$CLh = Qh \times (1\text{-}Fh) \qquad (3\text{-}6)'$$

$$Fh = 4a / (1+a)^2 \exp[(a-1)/2D_N] - (1-a)^2 \exp[-(a+1)/2D_N] \qquad (3\text{-}7)$$

$$a = [1+(4 \times fp/Rb \times CLint_{vivo} \times D_N /Qh)]^{1/2} \qquad (3\text{-}8)$$

where CLt, CLh, and CLr are total, hepatic, and renal clearance; fe is the ratio of the urinary excretion of unchanged drug; dose iv and AUC iv are dosage at intravenous administration and the area under the plasma concentration-time curve after intravenous administration, respectively; Fh is hepatic availability; Qh and D_N are hepatic blood flow rate and dispersion number, with values of 20.7 mL/min/kg and 0.17 used, respectively (Naritomi et al., 2003).

If iv data were not available, CLoral was used to calculate CLh using the following equation, after which CLint $_{vivo}$ was calculated by equations (3-7) and (3-8).

$$CLoral = CLh / (1\text{-}fe) \times Fa \times Fg \times Fh \qquad (3\text{-}9)$$

where Fa and Fg are fraction absorbed and intestinal availability, respectively (assumed to be 1 if data are not available)

I used the average values in subjects to calculate $CLint_{vivo}$. In cases where a parameter showed as a range of minimum to maximum in the literature, the intermediate value between the minimum and maximum, namely (minimum + maximum)/2, was used. In cases where data were not available, 70 kg was used for human body weight, CLr or fe were assumed to be 0, and Fa and Fg were assumed to be 1.

3.3 Results

3.3.1 *In vitro* intrinsic clearance in fresh and cryopreserved hepatocytes

$CLint_{vitro, hep}$ values of FK3453, O6BG, PHT, and ZAL in donor-matched fresh and cryopreserved hepatocytes were summarized in Figure 3-2 and Table 3-1. On direct comparison of $CLint_{vitro, hep}$ in freshly isolated and cryopreserved hepatocytes from the same donors (n = 4), I found that cryopreservation resulted in -32% to +85% changes in $CLint_{vitro, hep}$ values of FK3453, O6BG, PHT, and ZAL.

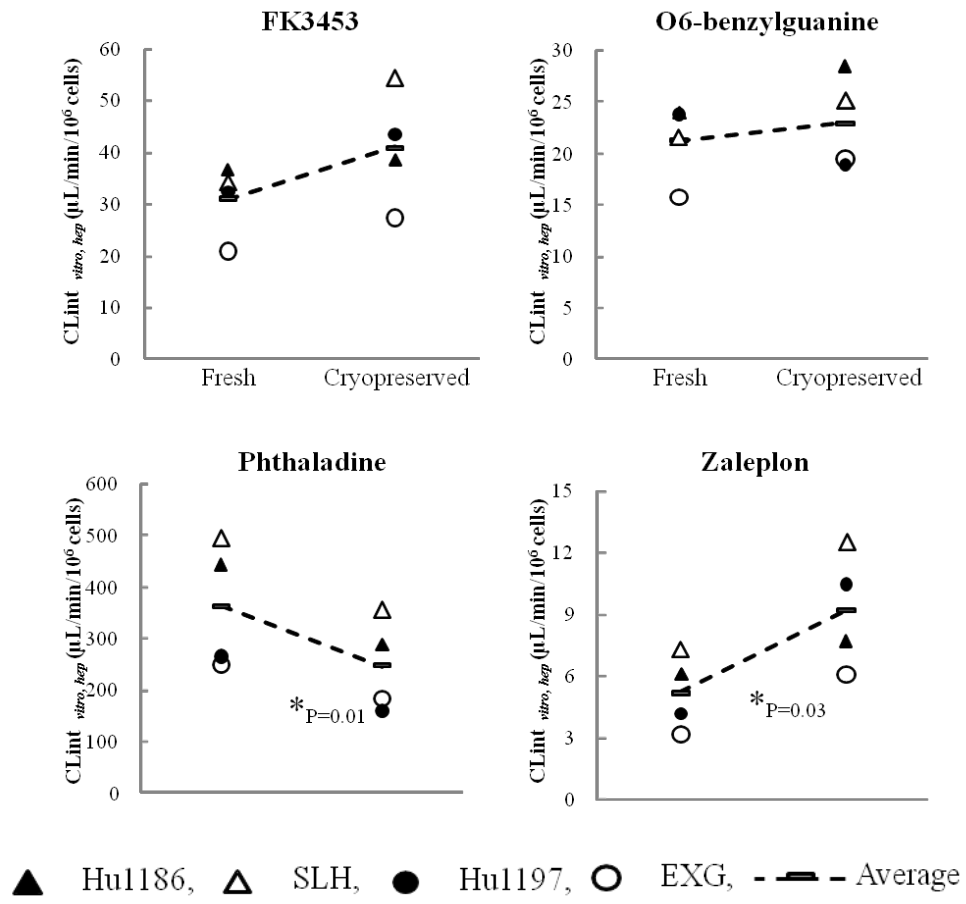

Figure 3-2. Comparison of AO enzyme activities of freshly isolated and cryopreserved hepatocytes from the same donor.

Closed triangle open triangle, closed circle, and open circle represent intrinsic clearance in Hu1186, SLH, Hu1197, and EXG, and bars represent mean value of intrinsic clearance in each compound.

TABLE 3-1 Summary of CLint $_{vitro, hep}$ in freshly isolated and cryopreserved human hepatocytes

Compounds	CLint $_{vitro, hep}$ (µL/min/10^6 cells)												Average Ratio (n=4)
	Hu1186			*SLH*			*Hu1193*			*EXG*			
	F	C	C/F	F	C	C/F	F	C	C/F	F	C	C/F	
FK3453	12.6	13.2	1.05	11.8	18.7	1.59	11.1	15	1.35	7.2	9.4	1.32	1.33
O6-benzylguanine	8.2	9.7	1.18	7.4	8.6	1.17	8.2	6.5	0.79	5.4	6.7	1.23	1.1
Phthalazine	152.9	99.6	0.65	169.8	122.4	0.72	91.6	54.9	0.6	85.8	63.2	0.74	0.68
Zaleplon	2.1	2.6	1.26	2.5	4.3	1.71	1.4	3.6	2.5	1.1	2.1	1.91	1.85

C, Cryopreserved hepatocytes; F, Fresh hepatocytes

3.3.2 *In vitro* intrinsic clearance in individual and pooled cryopreserved hepatocytes

The CLint $_{vitro,\ hep}$ values of FK3453, O6BG, and ZAL in individual hepatocytes and pooled hepatocytes are summarized in Figure 3-3 and Table 3-2. Values in pooled hepatocytes were +4%, +55%, and +7% of average clearance value in individual hepatocytes for FK3453, O6BG, and ZAL, respectively.

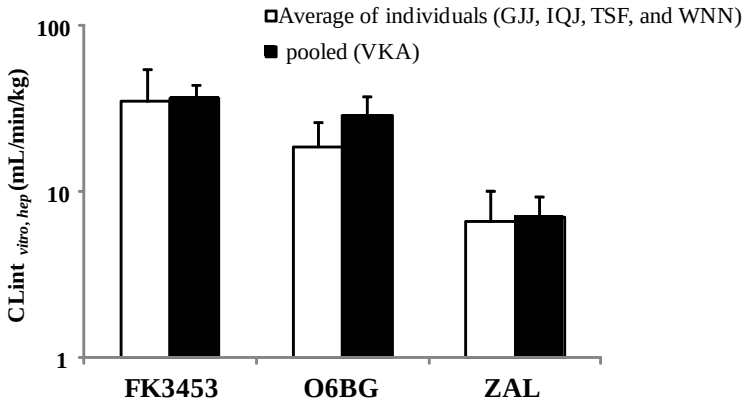

Figure 3-3. Comparison of intrinsic clearance in pooled (VKA) and individual cryopreserved hepatocytes (GGJ, IQJ, TSF, and WNN).

Open column represents intrinsic clearance in GGJ, IQJ, TSF, and WNN. Solid column represents mean value of intrinsic clearance in VKA (mean, n=3). Error bars represent the standard deviation.

TABLE 3-2. *In vitro* intrinsic clearance in individual and pooled hepatocytes.

Compound	Individual lots							VKA (mean±SD, n=3)			Ratio
	GGJ	IQJ	TSF	WNN	Mean	± SD	(CV)	Mean	± SD	(CV)	
	mL/min/kg						*%*	*mL/min/kg*		*%*	
FK3453	22.2	30.0	23.1	64.6	35.0	± 20.1	(57)	36.4	± 7.8	(21)	1.04
o6-benzylguanine	13.7	22.2	11.4	27.7	18.8	± 7.5	(40)	29.1	± 8.6	(30)	1.55
zaleplon	3.4	5.9	5.2	11.8	6.6	± 3.7	(56)	7.1	± 2.3	(32)	1.07

GGJ, IQJ, TSF, WNN and VKA, lot names of individual hepatocytes and pooled hepatocytes; Ratio, average value of CLint in VKA per that in individuals (GGJ, IQJ, TSF, and WNN).

3.3.3 *In vitro-in vivo* correlation analysis using pooled cryopreserved hepatocytes

Rb, fp and fu $_{hep}$ in AO substrates

Rb, fp, and fu $_{hep}$ values in AO-cleared compounds are listed in Table 3-3. An extremely high value of protein binding was observed in XK (99.3%).

TABLE 3-3. Summary of blood-to-plasma concentration ratio, protein binding, and unbound fraction in hepatocyte incubation of AO substrates

	Rb	fp	fu$_{, hep}$
FK3453	0.86	0.195	0.90
o^6-benzylguanine	1.02	0.086	0.85
zaleplon	0.92	0.402	0.83
6-deoxypenciclovir	1.08	0.793	0.99
XK-469	0.55 [a]	0.007 [b]	0.98
zoniporide	0.81	0.320	0.89

Rb, blood to plasma concentration ratio; fp, unbound drug fraction in plasma; fu $_{hep}$, unbound fraction in hepatocyte incubation.

[a] Assumed to be 0.55 (calculated values were below 0.55).

[b] Rapid equilibrium dialysis was used for determination.

In vitro-in vivo *correlation of CLint* $_{vivo}$ *and CLint* $_{vitro}$

Values overall showed a trend toward underestimation. Underestimation was approximately 10-fold (7.2- to 14.9-fold) for all AO substrate compounds (Fig.3-4, Table 3-4).

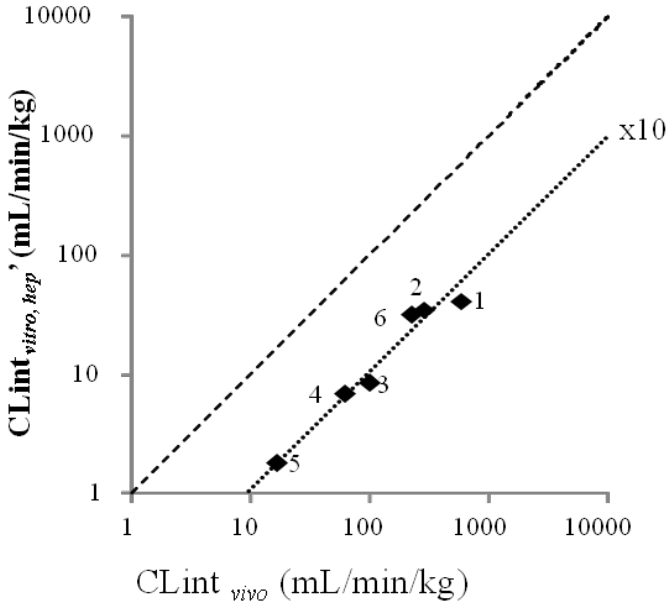

Figure 3-4. *In vitro-in vivo* correlation analysis for AO substrates.

1, FK3453; 2, o^6-benzylguanine; 3, zaleplon; 4, 6-deoxypenciclovir; 5, XK-469; and 6, zoniporide.

TABLE 3-4. Summary of *in vitro* intrinsic clearance in VKA and *in vivo* intrinsic clearance.

Compound	VKA (Mean±SD, n=3)			*In vivo* parameters					
	CLint $_{vitro, hep}$ mL/min/kg	(CV) %	CLint $_{vitro, hep}$ '	CLt or CLoral mL/min/kg	CLint $_{vivo}$	fe (%)	Fa	Reference
FK3453	36.4 ± 7.8	(21)	40.4	1087 [a]	603.2	0	1	See Chapter 2
o^6-benzylguanine	29.1 ± 8.6	(30)	34.3	13.6	288.9	0 [b]	-	Tserng et al., 2003
zaleplon	7.1 ± 2.3	(32)	8.5	15.7	102.3	0	-	Rosen et al., 1999
6-deoxypenciclovir	6.7 ± 1.8	(26)	6.9	118 [a,c]	63.6	-	-	Zientek et al., 2010
XK-469	1.8 ± 0.4	(24)	1.8	0.12	16.9	2	-	Alousi et al., 2007
zoniporide	28.2 ± 2.8	(10)	31.6	21	227.8 [d)]	-	-	Zientek et al., 2010

CLint $_{vitro, hep}$ ', *in vitro* intrinsic clearance divided by unbound fraction in hepatocyte incubation (fu $_{hep}$)

[a] CLoral

[b] Assumed to be 0.

[c] Assuming all dosed famciclovir is converted to 6-deoxypenciclovir (Zientek et al., 2010)

[d] CLint $_{vivo}$ was cited from Zientek et al., 2010 and corrected by the contribution ratio of aldehyde oxidase metabolism to total elimination.

3.4Discussion

Here, to examine the usefulness of human hepatocytes as an evaluation tool for AO substrate compounds in drug discovery, potential effects of cryopreservation on AO enzyme activities was assessed by comparing $CLint_{vitro, hep}$ values in FK3453, O6BG, PHT, and ZAL which are reported to be primarily metabolized by AO in humans between freshly isolated and cryopreserved hepatocytes.

Subsequently, I compared AO enzyme activity in four lots of cryopreserved hepatocytes from individuals (GGJ, IQJ, TSF, and WNN) with that in a custom pooled lot (VKA) made from those same individual lots using FK3453, O6BG, and ZAL. IVIVC analysis for hepatic clearance prediction was then performed in 6 AO-cleared compounds by comparing $CLint_{vitro, hep}$ in pooled hepatocytes (lot name: VKA) and $CLint_{vivo}$ were obtained from clinical data in the literature.

Effect of cryopreservation on AO enzyme activities in hepatocytes

In the present study, I evaluated the effect of cryopreservation on AO in two ways: direct comparison of AO enzyme activities between freshly isolated and cryopreserved human hepatocytes from the same donor (n=4), and between individual lots and in pooled hepatocytes consisting of lots from the same individual donors.

I investigated the effects of cryopreservation by comparing $CLint_{vitro, hep}$ values for FK3453, O6BG, PHT, and ZAL in four pairs of fresh and cryopreserved hepatocytes derived from the same donors (Hu1086, Hu1097, EXG, and SLH, Fig. 3-2, Table 3-1). Although I observed a significant

reduction in $CLint_{vitro,\ hep}$ for PHT after cryopreservation when compared to donor-matched fresh hepatocytes (−32%), the changes in $CLint_{vitro,\ hep}$ values after cryopreservation were within 2-fold in all AO substrates (+33%, +10%, and +85% for FK3453, O6BG, and ZAL, respectively).

On comparison of average $CLint_{vitro,\ hep}$ values between individual and pooled hepatocytes for FK3453, O6BG, and ZAL, $CLint_{vitro,\ hep}$ values in custom pooled hepatocytes showed +4%, +55%, and +7% of average clearance in individual hepatocytes, respectively. These data support the idea that pooled hepatocytes reflect the mean value of metabolic activities of each individual lot which contribute to the pool. Further, AO enzymes activity maintained during the freezing and thawing process generally required for pooled hepatocytes. These results indicated that pooled human hepatocytes are a useful tool in evaluating AO metabolism in large-scale compound screening.

In vitro-in vivo *correlation for AO substrates*

IVIVC analysis for AO-cleared compounds was then performed by comparing $CLint_{vitro,\ hep}$ in pooled hepatocytes and $CLint_{vivo}$ calculated from previously published clinical data.

In this study, although the rank order of $CLint_{vitro,\ hep}$ with $CLint_{vivo}$ was maintained, 7.9- to 14.9-fold underestimation was observed in IVIVC for all 6 AO substrates (Fig. 3-3). Given that a similar range of under-prediction (average 11-fold) was also observed in predicting human *in vivo* clearance from $CLint_{vitro}$ calculated from cytosol or S9 (Zientek et al. 2010), the risk of underestimation of AO metabolism in humans exists regardless of enzyme resource. In general, not only with AO, it is known that the $CLint_{vitro}$ obtained from human liver microsomes or hepatocytes

systematically under-predicted $CLint_{vivo}$ by 9 and 3-6-fold, respectively (Chiba et al., 2009). Several interesting recent papers might potentially explain the under-prediction in several category compounds based on mechanistic rationales. For example, the prediction method of Poulin et al improved prediction accuracy in highly protein binding compounds which showed a tendency to the underestimation of predicted clearance by conventional method (Poulin et al., 2012). Prediction of clearance of acid compounds, whose clearance was under-predicted from hepatic metabolism parameter only, was improved by including hepatic uptake, biliary excretion, and sinusoidal efflux into the clearance calculation (Umehara and Camenish, 2012). Unfortunately, these strategies may not be directly applicable to the AO substrates tested in this study, as most of them are basic compounds (Fig. 3-1) and show moderate protein binding except XK-469 (Table 3-3). While the reason for this consistent underestimation of AO metabolism in humans remains unclear, Zientek et al (2010) suggested several possibilities, including the contribution of extra-hepatic metabolism to total clearance and enzyme lability during preparation or storage. Likewise, Chiba et al (2009) also discussed possible reasons for underestimation of $CLint_{vivo}$ saying that extrinsic factors such as preparation process and storage conditions are responsible for the potential loss of enzyme activity in human liver extracts or hepatocytes, resulting in the systematic under-prediction. However, evaluation of AO activity using fresh human liver biopsy after harvesting is almost impossible, therefore, I cannot assess the lability issues using human sample. One possibility might be the use of monkeys as a preclinical species for assessing AO metabolism, given their high reported AO activity (Diamond et al., 2010). Evaluation of AO lability during preparation or storage might be

assessed by comparing AO activity between liver biopsy immediately after harvesting and hepatocytes in monkeys. Meanwhile, underestimation at a constant rate, as observed in this study, suggests the possibility that prediction accuracy may be improved by using an empirical scaling factor. I propose that the $CLint_{vivo}$ may be well predicted by calculating the geometric average ratio of $CLint_{vivo}$ / $CLint_{vitro, hep}$ from several reference drugs as a scaling factor, and then multiplying $CLint_{vitro, hep}$ of the candidate by that scaling factor. Using the 6 AO substrates tested in this study as examples, empirical scaling factors of 9.1 to 10.6 were calculated using the other 5 substrates, and $CLint_{vivo}$ was predicted to be within 2-fold in all tested compounds (Table 3-5). With regard to FK3453, CLh was calculated to be 19.5 mL/min/kg from 369.3 of predicted $CLint_{vivo}$ by the dispersion model. These results confirm the observed poor human exposure of FK3453, and also confirm that this poor exposure risk would have been identified if hepatocytes had been used as a screening tool. A similar approach was taken by Hutzler et al (2012), who predicted hepatic clearance from a well-stir model using human cryopreserved hepatocytes with several AO substrates including BIBX1382, which had been expected to show acceptable exposure in humans from pre-clinical data, but in fact showed less than 5% of BA in humans. They confirmed that the risk of high clearance in BIBX1382 due to AO metabolism would be detected if the predicted hepatic clearance from cryopreserved hepatocytes was used to estimate BA in humans. By comparison, use of the well-stir model in IVIVC analysis for the 6 compounds in this study resulted in non-constant under-prediction compared to the dispersion model, which is not adequate for empirical scaling theory, as described above. The underestimation ratio increased proportionally

with $CLint_{vivo}$ in well-stir model-based analysis (data not shown); however, these model-depend difference may be explained by the mathematical theory in both models. If $CLint_{vivo}$ is calculated back from CLh or CLoral, the $CLint_{vivo}$ value from a well-stirred model is higher than that from the dispersion model, especially with high-clearance drugs (Chiba et al., 2009).

These observations further suggest the possibility that relatively large pools of hepatocytes with superior AO enzyme activities might be obtained by selecting individual lots following preliminary characterization. As previously reported by Shibata et al (2002), who reported successful quantitative clearance prediction using 14 drugs mainly metabolized by CYP, hepatic clearance prediction for AO metabolism within a certain period of time would be made possible using custom pooled hepatocytes from several individuals whose hepatocytes had been pre-identified as showing good IVIVC for AO substrate drugs.

TABLE 3-5. Prediction of hepatic clearance of AO compounds using an empirical scaling factor.

Compound	Observed			Predicted	
	$CLint_{vivo}$	$CLint_{vitro, hep}'$	Ratio	ESF	CLint pred
FK3453	603.2	40.4	14.9	9.1	369.3
o6-benzylguanine	288.9	34.3	8.4	10.2	351.2
zaleplon	102.3	8.5	12.1	9.5	80.7
6-deoxypenciclovir	63.6	6.9	9.3	10.1	69.2
XK-469	16.9	1.8	9.4	10.0	18.0
zoniporide	227.8	31.6	7.2	10.6	334.5

$CLint_{vitro, hep}'$, *in vitro* intrinsic clearance divided by unbound fraction in hepatocyte incubation (fu_{hep}); Ratio, $CLint_{vivo}$ / $CLint_{vitro, hep}'$; ESF, empirical scaling factor (geometric mean of $CLint_{vivo}$/ $CLint_{vitro, hep}'$ in other 5 substrates: e.g. 9.1 in FK3453 responds to the geometric mean of 8.4, 12.1, 9.3, 9.4, and 7.2 in o6-benzylguanine, zaleplon, 6-deoxypenciclovir, XK-469, and zoniporide); $CLint_{pred}$, predicted intrinsic clearance: $CLint_{vitro, hep}'$× ESF.

In conclusion, pooled hepatocytes reflect the average of the AO enzyme activities of the individual hepatocytes used to make the pool. This observation enabled us to obtain specific pooled hepatocytes which showed the expected AO enzyme activities by pre-characterization. While a trend toward underestimation was observed in IVIVC analysis for AO metabolism using hepatocytes, I successfully quantified the hepatic clearance prediction for these compounds using an empirical scaling factor.

Concluding Remarks

Summary of the studies

Commercialization of human liver microsomes and the development of methods for predicting human hepatic CYP metabolism have enabled selection of candidates stable against CYP metabolism in the early drug discovery stage. However, extra-hepatic and non-CYP metabolism continue to pose problems with human pharmacokinetic prediction for drug candidates. Here, I have described the impacts of species differences in intestinal metabolism and AO metabolism on human pharmacokinetic prediction in drug discovery. In addition, I also discussed a novel approach to quantitate human hepatic clearance by AO metabolism.

In Chapter 1, I demonstrated the risk of underestimating human BA prediction in drug discovery research and discussed the importance of separate evaluation of Fa, Fg, and Fh when predicting human BA from monkey pharmacokinetic parameters. In addition, the potential of such novel approaches to estimating Fg values in humans was nevertheless suggested.

On comparing BA, Fh, and FaFg after intravenous and oral administrations of 13 commercially available drugs to cynomolgus monkeys with those for humans reported in the literatures, 8 of 13 drugs showed markedly lower BA in monkeys than those in humans. There were no obvious differences in Fh between humans and monkeys, however, a remarkable species difference in FaFg was observed. Given that *in vitro* membrane permeability data suggested favorable Fa in monkeys

for all tested drugs, higher first-pass intestinal metabolism in cynomolgus monkeys than in humans was suggested as a major factor of the markedly lower BA observed in monkeys. $CLint_{vitro}$ values were larger in monkey intestinal microsomes than in humans for 5 of the 8 drugs which showed low BA in monkeys, suggesting that species difference in intestinal metabolism between humans and monkeys results in drastic underestimation of human BA, thereby leading to a loss of candidates with favorable pharmacokinetic profiles in humans in drug discovery research. As cynomolgus monkeys are widely used in pharmacokinetic and drug-safety studies, separate evaluation of FaFg and Fh is recommended when using monkey pharmacokinetic parameters for candidate selection. In addition, a metabolic stability assay using human intestine microsomes may help to better understand pharmacokinetic profiles of drug candidates in humans.

In Chapter 2, the risk of extensive AO metabolism in humans was discussed by describing preclinical and clinical pharmacokinetic profiles of FK3453 and the mechanism responsible for poor oral exposure of FK3453 in humans. Although FK3453 showed a promising pharmacokinetic profile in preclinical studies, such as demonstrating a satisfactory BA, total body clearance in animals, and favorable metabolic stability in liver microsomes, plasma concentrations of FK3453 in humans were extremely low, with M4 identified as a major metabolite. AO was identified as the enzyme responsible for poor exposure of FK3453 in humans by *in vitro* metabolic study using human liver sub-cellular fractions such as S9, cytosol, and microsomes with or without inhibitors. While rats and dogs have also been widely used for preclinical studies for drug development at

pharmaceutical industries, rat- and dog-based pharmacokinetic studies and microsome-based compound screening are not sufficiently capable of evaluating the *in vitro-in vivo* relationship for AO metabolism and predicting the human pharmacokinetic profile. As such, great care must be taken to avoid candidate attrition in human pharmacokinetic studies should the candidate be metabolized by AO.

In Chapter 3, I verified that findings in pooled hepatocytes represent the average of the AO enzyme activities of the individual hepatocytes. A quantitative method of predicting hepatic AO metabolism in humans using pooled hepatocytes was also developed to avoid the risk of underestimating AO metabolism in humans. Although pooled cryopreserved hepatocytes were believed to be the most efficient tool in evaluating AO metabolism during drug discovery research, considering their advantages in usability, whether or not the process of producing pooled hepatocytes, which involves at least two rounds of freezing and thawing, adversely affected AO activity remained unclear. Consequently, $CLint_{vitro,\ hep}$ values of AO-cleared compounds in human hepatocytes were maintained among fresh, cryopreserved, and pooled hepatocytes.

Given the above results, pooled hepatocytes were selected for IVIVC analysis to predict hepatic clearance of AO-cleared compounds in humans. Although approximately 10-fold underestimation was observed in IVIVC analysis using pooled hepatocytes for all tested AO substrates, quantitative hepatic clearance for AO compounds was successfully predicted with an empirical scaling factor. I also confirmed that the poor exposure risk of FK3453 in humans would

have been identified if hepatocytes had been used as a screening tool.

Taken together, these present findings allowed us to avoid passing over potential candidates with acceptable pharmacokinetic profile in humans due to intestinal metabolism and candidate attrition during phase 1 trials due to unexpected high AO metabolism in humans, thereby facilitating more efficient candidate selection and optimization in drug discovery research.

Future prospects

In future studies, I would like to thoroughly examine the usefulness of a monkey pharmacokinetic profile of AO substrates in evaluating AO metabolism for drug discovery, as high AO activity has been reported in monkeys. And if monkey represents higher AO activity in humans, in-depth studies regarding elimination pathway such as contribution of intestinal CYP or AO will be required to estimate human BA of new chemical entities in cases where the compound shows favorable pharmacokinetic profiles in rats and dogs but markedly poor exposure in monkeys.

Subsequently, while a quantitative approach using intestinal microsomes was suggested in Chapter 1, this study doesn't describe Fg in humans directly. Development of a mathematical model to calculate Fg value from *in vitro* data will be useful for adequate candidate selection. In addition, the AO-specific underestimation could be overcome using ESF, provided the compounds are mainly metabolized by AO (Chapter 3); however, methods of estimating the hepatic clearance of compounds in which AO only partially contributes to their elimination from the body remain to be developed.

In the future, I expect more factors besides intestinal or AO metabolism with a crucial impact on human BA prediction to be identified. In the present study, investigations into the cause of low BA or the establishment of evaluation systems to complement these factors were shown to be important in furthering pharmacokinetic research in drug discovery.

References

Alousi AM, Boinpally R, Wiegand R, Parchment R, Gadgeel S, Heilbrun LK, Wozniak AJ, DeLuca P, LoRusso PM: A phase 1 trial of XK469: toxicity profile of a selective topoisomerase IIbeta inhibitor. *Invest New Drugs* 2007, 25(2):147-154.

Arancibia A, Corvalan F, Mella F, Concha L: Absorption and disposition kinetics of lithium carbonate following administration of conventional and controlled release formulations. *Int J Clin Pharmacol Ther Toxicol* 1986, 24(5):240-245.

Avdeef A, Artursson P, Neuhoff S, Lazorova L, Grasjo J, Tavelin S: Caco-2 permeability of weakly basic drugs predicted with the double-sink PAMPA pKa(flux) method. *Eur J Pharm Sci* 2005, 24(4):333-349.

Beedham C: Molybdenum hydroxylases: biological distribution and substrate-inhibitor specificity. *Prog Med Chem* 1987, 24:85-127.

Beedham C, Miceli JJ, Obach RS: Ziprasidone metabolism, aldehyde oxidase, and clinical implications. *J Clin Psychopharmacol* 2003, 23(3):229-232.

Benet LZ, Izumi T, Zhang Y, Silverman JA, Wacher VJ: Intestinal MDR transport proteins and P-450 enzymes as barriers to oral drug delivery. *J Control Release* 1999, 62(1-2):25-31.

Borgstrom L, Johansson CG, Larsson H, Lenander R: Pharmacokinetics of propranolol. *J Pharmacokinet Biopharm* 1981, 9(4):419-429.

Chiba M, Hensleigh M, Lin JH: Hepatic and intestinal metabolism of indinavir, an HIV protease inhibitor, in rat and human microsomes. Major role of CYP3A. *Biochem Pharmacol* 1997, 53(8):1187-1195.

Chiba M, Ishii Y, Sugiyama Y: Prediction of hepatic clearance in human from in vitro data for successful drug development. *AAPS J* 2009, 11(2):262-276.

Chiou WL, Buehler PW: Comparison of oral absorption and bioavailablity of drugs between monkey and human. *Pharm Res* 2002, 19(6):868-874.

Dalvie D, Zhang C, Chen W, Smolarek T, Obach RS, Loi CM: Cross-species comparison of the metabolism and excretion of zoniporide: contribution of aldehyde oxidase to interspecies differences. *Drug Metab Dispos* 2010, 38(4):641-654.

Davies B, Morris T: Physiological parameters in laboratory animals and humans. *Pharm Res* 1993, 10(7):1093-1095.

De Buck SS, Sinha VK, Fenu LA, Nijsen MJ, Mackie CE, Gilissen RA: Prediction of human pharmacokinetics using physiologically based modeling: a retrospective analysis of 26 clinically tested drugs. *Drug Metab Dispos* 2007, 35(10):1766-1780.

Diamond S, Boer J, Maduskuie TP, Jr., Falahatpisheh N, Li Y, Yeleswaram S: Species-specific metabolism of SGX523 by aldehyde oxidase and the toxicological implications. *Drug Metab Dispos* 2010, 38(8):1277-1285.

Doherty MM, Charman WN: The mucosa of the small intestine: how clinically relevant as an organ of drug metabolism? *Clin Pharmacokinet* 2002, 41(4):235-253.

Duggan DE, Yeh KC, Matalia N, Ditzler CA, McMahon FG: Bioavailability of oral dexamethasone. *Clin Pharmacol Ther* 1975, 18(2):205-209.

Evans GH, Nies AS, Shand DG: The disposition of propranolol. 3. Decreased half-life and volume of distribution as a result of plasma binding in man, monkey, dog and rat. *J Pharmacol Exp Ther* 1973, 186(1):114-122.

Fagerholm U: Prediction of human pharmacokinetics--gut-wall metabolism. *J Pharm Pharmacol* 2007, 59(10):1335-1343.

Fisher MB, Labissiere G: The role of the intestine in drug metabolism and pharmacokinetics: an industry perspective. *Curr Drug Metab* 2007, 8(7):694-699.

Greenblatt DJ, Pfeifer HJ, Ochs HR, Franke K, MacLaughlin DS, Smith TW, Koch-Weser J: Pharmacokinetics of quinidine in humans after intravenous, intramuscular and oral administration. *J Pharmacol Exp Ther* 1977, 202(2):365-378.

Hinderling PH, Hartmann D: Pharmacokinetics of digoxin and main metabolites/derivatives in healthy humans. *Ther Drug Monit* 1991, 13(5):381-401.

Holtbecker N, Fromm MF, Kroemer HK, Ohnhaus EE, Heidemann H: The nifedipine-rifampin interaction. Evidence for induction of gut wall metabolism. *Drug Metab Dispos* 1996, 24(10):1121-1123.

Hutzler JM, Yang YS, Albaugh D, Fullenwider CL, Schmenk J, Fisher MB: Characterization of aldehyde oxidase enzyme activity in cryopreserved human hepatocytes. *Drug Metab Dispos* 2012, 40(2):267-275.

Itoh K, Maruyama H, Adachi M, Hoshino K, Watanabe N, Tanaka Y: Lack of formation of aldehyde oxidase dimer possibly due to 377G>A nucleotide substitution. *Drug Metab Dispos* 2007, 35(10):1860-1864.

Itoh K, Maruyama H, Adachi M, Hoshino K, Watanabe N, Tanaka Y: Lack of dimer formation ability in rat strains with low aldehyde oxidase activity. *Xenobiotica* 2007, 37(7):709-716.

Iwatsubo T, Hirota N, Ooie T, Suzuki H, Sugiyama Y: Prediction of in vivo drug disposition from in vitro data based on physiological pharmacokinetics. *Biopharm Drug Dispos* 1996, 17(4):273-310.

Johns DG: Human liver aldehyde oxidase: differential inhibition of oxidation of charged and uncharged substrates. *J Clin Invest* 1967, 46(9):1492-1505.

Kadono K, Akabane T, Tabata K, Gato K, Terashita S, Teramura T: Quantitative prediction of intestinal metabolism in humans from a simplified intestinal availability model and empirical scaling factor. *Drug Metab Dispos* 2010, 38(7):1230-1237.

Kawashima K, Hosoi K, Naruke T, Shiba T, Kitamura M, Watabe T: Aldehyde oxidase-dependent marked species difference in hepatic metabolism of the sedative-hypnotic, zaleplon, between monkeys and rats. *Drug Metab Dispos* 1999, 27(3):422-428.

Kitamura S, Sugihara K, Nakatani K, Ohta S, Ohhara T, Ninomiya S, Green CE, Tyson CA: Variation of hepatic methotrexate 7-hydroxylase activity in animals and humans. *IUBMB Life* 1999, 48(6):607-611.

Kitamura S, Sugihara K, Ohta S: Drug-metabolizing ability of molybdenum hydroxylases. *Drug Metab Pharmacokinet* 2006, 21(2):83-98.

Kivisto KT, Niemi M, Fromm MF: Functional interaction of intestinal CYP3A4 and P-glycoprotein. *Fundam Clin Pharmacol* 2004, 18(6):621-626.

Kola I, Landis J: Can the pharmaceutical industry reduce attrition rates? *Nat Rev Drug Discov* 2004, 3(8):711-715.

Li AP: Human hepatocytes: isolation, cryopreservation and applications in drug development. *Chem Biol Interact* 2007, 168(1):16-29.

Li AP: Evaluation of drug metabolism, drug-drug interactions, and in vitro hepatotoxicity with cryopreserved human hepatocytes. *Methods Mol Biol* 2010, 640:281-294.

Martin W, Koselowske G, Toberich H, Kerkmann T, Mangold B, Augustin J: Pharmacokinetics and absolute bioavailability of ibuprofen after oral administration of ibuprofen lysine in man. *Biopharm Drug Dispos* 1990, 11(3):265-278.

Massey V, Komai H, Palmer G, Elion GB: On the mechanism of inactivation of xanthine oxidase by allopurinol and other pyrazolo[3,4-d]pyrimidines. *J Biol Chem* 1970, 245(11):2837-2844.

McAllister RG, Jr., Kirsten EB: The pharmacology of verapamil. IV. Kinetic and dynamic effects after single intravenous and oral doses. *Clin Pharmacol Ther* 1982, 31(4):418-426.

Mihara T, Iwashita A, Matsuoka N: A novel adenosine A(1) and A(2A) receptor antagonist ASP5854 ameliorates motor impairment in MPTP-treated marmosets: comparison with existing anti-Parkinson's disease drugs. *Behav Brain Res* 2008, 194(2):152-161.

Mihara T, Mihara K, Yarimizu J, Mitani Y, Matsuda R, Yamamoto H, Aoki S, Akahane A, Iwashita A, Matsuoka N: Pharmacological characterization of a novel, potent adenosine A1 and A2A receptor dual antagonist, 5-[5-amino-3-(4-fluorophenyl)pyrazin-2-yl]-1-isopropylpyridine-2(1H)-one (ASP5854), in models of Parkinson's disease and cognition. *J Pharmacol Exp Ther* 2007, 323(2):708-719.

Mihara T, Noda A, Arai H, Mihara K, Iwashita A, Murakami Y, Matsuya T, Miyoshi S, Nishimura S, Matsuoka N: Brain adenosine A2A receptor occupancy by a novel A1/A2A receptor antagonist, ASP5854, in rhesus monkeys: relationship to anticataleptic effect. *J Nucl Med* 2008, 49(7):1183-1188.

Moller A, Iwasaki K, Kawamura A, Teramura Y, Shiraga T, Hata T, Schafer A, Undre NA: The disposition of 14C-labeled tacrolimus after intravenous and oral administration in healthy human subjects. *Drug Metab Dispos* 1999, 27(6):633-636.

Mugford CA, Mortillo M, Mico BA, Tarloff JB: 1-Aminobenzotriazole-induced destruction of hepatic and renal cytochromes P450 in male Sprague-Dawley rats. *Fundam Appl Toxicol* 1992, 19(1):43-49.

Naritomi Y, Terashita S, Kagayama A, Sugiyama Y: Utility of hepatocytes in predicting drug metabolism: comparison of hepatic intrinsic clearance in rats and humans in vivo and in vitro. *Drug Metab Dispos* 2003, 31(5):580-588.

Naritomi Y, Terashita S, Kimura S, Suzuki A, Kagayama A, Sugiyama Y: Prediction of human hepatic clearance from in vivo animal experiments and in vitro metabolic studies with liver microsomes from animals and humans. *Drug Metab Dispos* 2001, 29(10):1316-1324.

Nassar AE, Kamel AM, Clarimont C: Improving the decision-making process in the structural modification of drug candidates: enhancing metabolic stability. *Drug Discov Today* 2004, 9(23):1020-1028.

Nishimura T, Amano N, Kubo Y, Ono M, Kato Y, Fujita H, Kimura Y, Tsuji A: Asymmetric intestinal first-pass metabolism causes minimal oral bioavailability of midazolam in cynomolgus monkey. *Drug Metab Dispos* 2007, 35(8):1275-1284.

Obach RS: Prediction of human clearance of twenty-nine drugs from hepatic microsomal intrinsic clearance data: An examination of in vitro half-life approach and nonspecific binding to microsomes. *Drug Metab Dispos* 1999, 27(11):1350-1359.

Ortiz de Montellano PR, Mathews JM: Autocatalytic alkylation of the cytochrome P-450 prosthetic haem group by 1-aminobenzotriazole. Isolation of an NN-bridged benzyne-protoporphyrin IX adduct. *Biochem J* 1981, 195(3):761-764.

Patel RB, Patel UR, Rogge MC, Shah VP, Prasad VK, Selen A, Welling PG: Bioavailability of hydrochlorothiazide from tablets and suspensions. *J Pharm Sci* 1984, 73(3):359-361.

Poulin P, Kenny JR, Hop CE, Haddad S: In vitro-in vivo extrapolation of clearance: modeling hepatic metabolic clearance of highly bound drugs and comparative assessment with existing calculation methods. *J Pharm Sci* 2012, 101(2):838-851.

Pybus J, Bowers GN, Jr.: Measurement of serum lithium by atomic absorption spectroscopy. *Clin Chem* 1970, 16(2):139-143.

Rosemond MJ, Walsh JS: Human carbonyl reduction pathways and a strategy for their study in vitro. *Drug Metab Rev* 2004, 36(2):335-361.

Rosen AS, Fournie P, Darwish M, Danjou P, Troy SM: Zaleplon pharmacokinetics and absolute bioavailability. *Biopharm Drug Dispos* 1999, 20(3):171-175.

Sakuda S, Akabane T, Teramura T: Marked species differences in the bioavailability of midazolam in cynomolgus monkeys and humans. *Xenobiotica* 2006, 36(4):331-340.

Sasaki T, Masubuchi A, Yamamura M, Watanabe N, Hiratsuka M, Mizugaki M, Itoh K, Tanaka Y: Rat strain differences in stereospecific 2-oxidation of RS-8359, a reversible and selective MAO-A inhibitor, by aldehyde oxidase. *Biopharm Drug Dispos* 2006, 27(5):247-255.

Schulz P, Turner-Tamiyasu K, Smith G, Giacomini KM, Blaschke TF: Amitriptyline disposition in young and elderly normal men. *Clin Pharmacol Ther* 1983, 33(3):360-366.

Shibata Y, Takahashi H, Chiba M, Ishii Y: Prediction of hepatic clearance and availability by cryopreserved human hepatocytes: an application of serum incubation method. *Drug Metab Dispos* 2002, 30(8):892-896.

Soars MG, McGinnity DF, Grime K, Riley RJ: The pivotal role of hepatocytes in drug discovery. *Chem Biol Interact* 2007, 168(1):2-15.

Soars MG, Webborn PJ, Riley RJ: Impact of hepatic uptake transporters on pharmacokinetics and drug-drug interactions: use of assays and models for decision making in the pharmaceutical industry. *Mol Pharm* 2009, 6(6):1662-1677.

Sugihara K, Kitamura S, Tatsumi K: Strain differences of liver aldehyde oxidase activity in rats. *Biochem Mol Biol Int* 1995, 37(5):861-869.

Tabata K, Hamakawa N, Sanoh S, Terashita S, Teramura T: Exploratory population pharmacokinetics (e-PPK) analysis for predicting human PK using exploratory ADME data during early drug discovery research. *Eur J Drug Metab Pharmacokinet* 2009, 34(2):117-128.

Takahashi M, Washio T, Suzuki N, Igeta K, Fujii Y, Hayashi M, Shirasaka Y, Yamashita S: Characterization of gastrointestinal drug absorption in cynomolgus monkeys. *Mol Pharm* 2008, 5(2):340-348.

Tamura K, Kobayashi M, Hashimoto K, Kojima K, Nagase K, Iwasaki K, Kaizu T, Tanaka H, Niwa M: A highly sensitive method to assay FK-506 levels in plasma. *Transplant Proc* 1987, 19(5 Suppl 6):23-29.

Thompson TN: Optimization of metabolic stability as a goal of modern drug design. *Med Res Rev* 2001, 21(5):412-449.

Thummel KE, O'Shea D, Paine MF, Shen DD, Kunze KL, Perkins JD, Wilkinson GR: Oral first-pass elimination of midazolam involves both gastrointestinal and hepatic CYP3A-mediated metabolism. *Clin Pharmacol Ther* 1996, 59(5):491-502.

Torres RA, Korzekwa KR, McMasters DR, Fandozzi CM, Jones JP: Use of density functional calculations to predict the regioselectivity of drugs and molecules metabolized by aldehyde oxidase. *J Med Chem* 2007, 50(19):4642-4647.

Tserng KY, Ingalls ST, Boczko EM, Spiro TP, Li X, Majka S, Gerson SL, Willson JK, Hoppel CL: Pharmacokinetics of O6-benzylguanine (NSC637037) and its metabolite, 8-oxo-O6-benzylguanine. *J Clin Pharmacol* 2003, 43(8):881-893.

Umehara K, Camenisch G: Novel in vitro-in vivo extrapolation (IVIVE) method to predict hepatic organ clearance in rat. *Pharm Res* 2012, 29(2):603-617.

Uno Y, Hosaka S, Matsuno K, Nakamura C, Kito G, Kamataki T, Nagata R: Characterization of cynomolgus monkey cytochrome P450 (CYP) cDNAs: is CYP2C76 the only monkey-specific CYP

gene responsible for species differences in drug metabolism? *Arch Biochem Biophys* 2007, 466(1):98-105.

Walle T, Fagan TC, Conradi EC, Walle UK, Gaffney TE: Presystemic and systemic glucuronidation of propranolol. *Clin Pharmacol Ther* 1979, 26(2):167-172.

Wallemacq PE, Firdaous I, Hassoun A: Improvement and assessment of enzyme-linked immunosorbent assay to detect low FK506 concentrations in plasma or whole blood within 6 hours. *Clin Chem* 1993, 39(6):1045-1049.

Waters NJ, Jones R, Williams G, Sohal B: Validation of a rapid equilibrium dialysis approach for the measurement of plasma protein binding. *J Pharm Sci* 2008, 97(10):4586-4595.

Williams JA, Hyland R, Jones BC, Smith DA, Hurst S, Goosen TC, Peterkin V, Koup JR, Ball SE: Drug-drug interactions for UDP-glucuronosyltransferase substrates: a pharmacokinetic explanation for typically observed low exposure (AUCi/AUC) ratios. *Drug Metab Dispos* 2004, 32(11):1201-1208.

Wilson TW, Firor WB, Johnson GE, Holmes GI, Tsianco MC, Huber PB, Davies RO: Timolol and propranolol: bioavailability, plasma concentrations, and beta blockade. *Clin Pharmacol Ther* 1982, 32(6):676-685.

Wishart DS: Improving early drug discovery through ADME modelling: an overview. *Drugs R D* 2007, 8(6):349-362.

Yang J, Jamei M, Yeo KR, Tucker GT, Rostami-Hodjegan A: Prediction of intestinal first-pass drug metabolism. *Curr Drug Metab* 2007, 8(7):676-684.

Yang XX, Hu ZP, Duan W, Zhu YZ, Zhou SF: Drug-herb interactions: eliminating toxicity with hard drug design. *Curr Pharm Des* 2006, 12(35):4649-4664.

Yu DK: The contribution of P-glycoprotein to pharmacokinetic drug-drug interactions. *J Clin Pharmacol* 1999, 39(12):1203-1211.

Zientek M, Jiang Y, Youdim K, Obach RS: In vitro-in vivo correlation for intrinsic clearance for drugs metabolized by human aldehyde oxidase. *Drug Metab Dispos* 2010, 38(8):1322-1327.

List of publications

1) Akabane T, Tabata K, Kadono K, Sakuda S, Terashita S, and Teramura T: A comparison of pharmacokinetics between humans and monkeys. *Drug Metab. Dispos*. 2010 **38**(2):308-316.

2) Akabane T, Tanaka K, Irie M, Terashita S, and Teramura T: Case report of extensive metabolism by aldehyde oxidase in humans: pharmacokinetics and metabolite profile of FK3453 in rats, dogs, and humans. *Xenobiotica* 2011 **41**(5):372-384.

3) Akabane T, Gerst N, Naritomi Y, Masters JN, and Tamura K: A practical and direct comparison of intrinsic metabolic clearance of several non-CYP enzyme substrates in freshly isolated and cryopreserved hepatocytes. *Drug Metab. Pharmacokinet*. 2012 **27**(2):181-191.

4) Akabane T, Gerst N, Masters JN, and Tamura K: A quantitative approach to hepatic clearance prediction of metabolism by aldehyde oxidase using custom pooled hepatocytes. *Xenobiotica* 2012 in Press.

Acknowledgement

I would like to thank sincerely Professor Kan Chiba, Chiba University, for providing the opportunity to take a doctorate. I would also like to express my sincere gratitude to his guidance and advices on this thesis and all of the manuscripts.

I would like to thank greatly Dr. Toshio Teramura, the Department Manager of Astellas Pharm Inc., for his support to this research.

I would like to thank deeply Dr. Kenji Tabata, Mr. Keitaro Kadono, Dr. Youichi Naritomi, Mr. Shuichi Sakuda, Dr. Megumi Irie, Mr. Koichiro Tanaka, and Dr. Shigeyuki Terashita of Astellas Pharm Inc., Nicolas Gerst, Jeffrey N Masters, and Kouichi Tamura of Astellas Research Institute of America LLC for their technical support and discussion for this research.

I would like to thank co-workers of Astellas Pharm Inc. and Astellas Research Institute of America LLC for their cooperation.

Finally I must thank my family for their patience and continued support.

Referees

This thesis for the doctorate was judged by the following referees authorized by the Graduate School of Pharmaceutical Sciences, Chiba University.

Dr. Kan Chiba, Professor, Chiba University,

School of Pharmaceutical Sciences - Chief referee

Dr. Toshihiko Toida, Professor, Chiba University,

School of Pharmaceutical Sciences

Dr. Toshiharu Horie, Professor, Chiba University,

School of Pharmaceutical Sciences

Dr. Toshihiko Murayama, Professor, Chiba University,

School of Pharmaceutical Sciences

Dr. Naoto Yamaguchi, Professor, Chiba University,

School of Pharmaceutical Sciences